FLUTTER CHARACTERISTICS OF PLATE LIKE STRUCTURES

A THESIS SUBMITTED TO THE GRADUATE SCHOOL OF NATURAL AND

APPLIED SCIENCES

OF

MIDDLE EAST TECHNICAL UNIVERSITY

BY

MEVLÜT BURAK DALMIŞ

IN PARTIAL FULFILLMENT OF THE REQUIREMENTS

FOR

THE DEGREE OF MASTER OF SCIENCE

IN

MECHANICAL ENGINEERING

NOVEMBER 2014

Approval of the thesis:

FLUTTER CHARACTERISTICS OF PLATE LIKE STRUCTURES

submitted by **MEVLÜT BURAK DALMIŞ** in partial fulfillment of the requirements for the degree of **Master of Science in Mechanical Engineering Department, Middle East Technical University** by,

Prof. Dr. Gülbin Dural Ünver _________________
Dean, **Graduate School of Natural and Applied Sciences**

Prof. Dr. R. Tuna Balkan _________________
Head of Department, **Mechanical Engineering**

Assist. Prof. Dr. Yiğit Yazıcıoğlu _________________
Supervisor, **Mechanical Engineering Dept., METU**

Burak Durak _________________
Co-Supervisor, **Structural and Mechanical Design Div., TÜBİTAK-SAGE**

Examining Committee Members:

Assoc. Prof. Dr. Ender Ciğeroğlu _________________
Mechanical Engineering Dept., METU

Assist. Prof. Dr. Yiğit Yazıcıoğlu _________________
Mechanical Engineering Dept., METU

Assoc. Prof. Dr. M. Metin Yavuz _________________
Mechanical Engineering Dept., METU

Assist. Prof. Dr. Ö. Uğraş Baran _________________
Mechanical Engineering Dept., TEDU

Burak Durak _________________
Structural and Mechanical Design Div., TÜBİTAK-SAGE

Date: _________________

I hereby declare that all information in this document has been obtained and presented in accordance with academic rules and ethical conduct. I also declare that, as required by these rules and conduct, I have fully cited and referenced all material and results that are not original to this work.

Name, Last name : Mevlüt Burak DALMIŞ

Signature :

ABSTRACT

FLUTTER CHARACTERISTICS OF PLATE LIKE STRUCTURES

Dalmış, Mevlüt Burak
M.S. Department of Mechanical Engineering
Supervisor: Asst. Prof. Dr. Yiğit Yazıcıoğlu
Co-Supervisor: Burak Durak

November 2014, 93 pages

In this study, flutter characteristics of plate like structures in incompressible flow are investigated by comparing the results of commercial flutter analysis program ZAERO© with wind tunnel tests conducted in Ankara Wind Tunnel (ART). Firstly, a rectangular polycarbonate (PC) plate, 5x125x1000 mm in dimensions, is investigated. In this case, analysis and test results are in good agreement with each other. Second test item is a 1/10 scaled F-16 wing like PC plate. In this case, the plate is capable of carrying external stores in different dimensions. Two different flutter analysis are conducted for this plate by using two different fixed end structural boundary conditions. In the first boundary condition, the plate is fixed from its bottom; in the second boundary condition, the plate is fixed from both bottom and side surfaces of the plate. Moreover, modal test is conducted by impact hammer for this test item. Results of this modal test indicates that modal analysis result using the first structural boundary condition, in which only bottom of the plate is fixed, is more realistic than the modal analysis result using the second structural boundary condition, in which the bottom of the plate with its side surfaces are kept fixed. Therefore, even if the modal analysis results are used for the flutter analysis, a modal test should be conducted in order to validate the modal analysis results to have accurate flutter analysis results. A comparison between two different solution methods of ZAERO©, namely K-method and g-method, is also done by using the results of second test item.

Key words: Flutter, ZAERO©, Plate, Flutter Analysis, Flutter Test, Wind Tunnel, Incompressible Flow

ÖZ

PLAKA BENZERİ YAPILARIN ÇIRPINTI KARAKTERİSTİKLERİ

Dalmış, Mevlüt Burak
Yüksek Lisans, Makine Mühendisliği Bölümü
Tez yöneticisi: Yrd. Doç. Dr. Yiğit Yazıcıoğlu
Ortak tez yöneticisi: Burak Durak

Kasım 2014, 93 sayfa

Bu çalışmada, plaka benzeri yapıların sıkıştırılamaz akıştaki çırpıntı karakteristikleri ticari çırpıntı analiz programı ZAERO© ile yapılan çırpıntı analizleri ile ART'de yapılan çırpıntı testleri sonuçlarının karşılaştırılması ile incelenmiştir. İlk olarak 5x125x1000 mm boyutlarında dikdörtgen polikarbonat plaka incelenmiştir. Bu durumda, analiz ve test sonuçları birbirleri ile uyumldur. İkinci test kalemi ise 1/10 ölçekli F-16 savaş uçağı boyutlarındaki PC plakadır. Bu durumda, plaka çeşitli boyutlardaki harici yükleri taşıyabilecek kabiliyettedir. Bu plaka için yapısal ankastre sınır koşulunu iki farklı biçimde modellemek suretiyle iki farklı çırpıntı analizi yapılmıştır. İlk sınır koşulunda plaka alt tarafından sabitlenmiştir, ikinci sınır koşulunda ise plaka hem alt tarafından hem de kenar yüzeylerinden sabitlenmiştir. Ayrıca bu test kalemi için darbe çekici ile modal test yapılmıştır. Modal test sonuçları plakanın sadece alt kısmının sabitlendiği ilk yapısal sınır koşulu ile yapılan modal analiz sonuçlarının plakanın alt kısmının yan yüzeyleri ile birlikte sabitlendiği ikinci yapısal sınır koşulu ile yapılanlara kıyasla daha gerçekçi olduğunu göstermektedir. Bu sebeple, çırpıntı analizinde modal analiz sonuçları kullanılacaksa bile, daha kesin çırpıntı analiz sonuçları elde etmek için modal analiz sonuçlarını doğrulayacak bir modal test yapılmalıdır. Bu plakanın sonuçları kullanılarak ZAERO©'nun iki farklı çözüm metodu da, K-metod ve g-metod, karşılaştırılmıştır.

Anahtar kelimeler: Çırpıntı, ZAERO©, Plaka, Çırpıntı Analizi, Çırpıntı Testi, Rüzgar Tüneli, Sıkıştırılamaz Akış

To My Family

ACKNOWLEDGEMENTS

I would like to express my sincere appreciation to my supervisor Dr. Yiğit Yazıcıoğlu and to my co-supervisor Mr. Burak Durak for their guidance in the preparation of this thesis.

The work in this thesis was performed for the practical research objectives of TÜBİTAK-SAGE (The Scientific and Technological Research Council of Turkey-Defense Industries Research and Development Institute). I wish to thank to TÜBİTAK-SAGE administration for allowing me to make this investigation and for unfolding the computational and testing capabilities. I would like to extend my special thanks to Mrs. Özlem Sümer, Mr. Taylan Karağaçlı, Mr. Muhammed Emin Cerit, Mr. Emre Okur, and Mr. Ahmet Ünal for their cooperation in testing and programming stages. I am also grateful to Mr. Kemal Yaman, Mr. Engin Metin Kaplan, and Mr. Tayfun Çelik for their support to motivate me in order to complete my studies.

I am especially grateful to my parents Şerife Dalmış and Abdullah Dalmış, my brothers Kadri Taha Dalmış and Sacit Alp Dalmış and also my sister Şerife Dalmış for their endless support during my studies.

Finally, I am thankful to a very valuable person for me, Havva Elif Doğan, due to her motivation through the end of my study. I wish her a successful and very happy life in the future.

TABLE OF CONTENTS

LIST OF TABLES

TABLES

LIST OF FIGURES

FIGURES

LIST OF ABBREVIATIONS

ART	:	Ankara Wind Tunnel
PC	:	Polycarbonate
GVT	:	Ground Vibration Testing
DoF	:	Degrees of freedom
PCM	:	Pulse code modulation
AIC	:	Aerodynamic Influence Coefficient
TÜBİTAK	:	The Scientific and Technological Research Council of Turkey
SAGE	:	Defense Industries Research and Development Institute
FE	:	Finite Element

LIST OF SYMBOLS

$[M_{GG}]$	:	Generalized mass matrix generated by structural FE-model
$[K_{GG}]$	:	Generalized stiffness matrix generated by structural FE-model
$\{x(t)\}$	:	Structural deformation
$\{\ddot{x}(t)\}$	:	Second derivative of the structural deformation
$\{F(t)\}$	:	Aerodynamic forces applied on the structure
$\{F_a(t)\}$	:	Aerodynamic forces induced by the structural deformation
$\{F_e(t)\}$	:	External forces
q_∞	:	Aerodynamic pressure
L	:	Reference length
c	:	Reference chord length
V	:	Velocity of the undisturbed flow
k	:	Reduced frequency
$[\Phi]$	:	Truncated modal matrix
$\{\mathrm{q(s)}\}$	:	Generalized coordinates, i.e. Modal coordinates.
$[M_{HH}]$	:	Generalized (modal) mass matrix
$[K]$	:	Generalized (modal) stiffness matrix
ω	:	Harmonic oscillatory frequency
$\{h\}$	:	Structural deformation defined at the aerodynamic boxes
$\{F_h\}$	:	Resultant aerodynamic forces at the aerodynamic boxes due to $\{h\}$
$\{\delta h\}$	:	Virtual displacement
$\{\delta x\}$	:	Virtual displacement
γ	:	Transient decay rate coefficient

CHAPTER 1

INTRODUCTION

1.1. General Introduction

Design of a new air vehicle or a new external store for an existing air vehicle is a complicated design task. That design task gets more complicated since more complex systems are desired by the consumers as a result of rapid progress in the engineering technology. It is also expected to decrease the design cost of these new products since the cost is always an important design consideration. Another important design consideration is time. Generally, limited time exists for research and development of a new product. MIL-HDBK-1763 “Aircraft/Stores Compatibility Systems Engineering Data Requirements and Test Procedures” explains how to certify a newly developed military aircraft or a new external store for an existing combat aircraft. Some of the tests designated in this handbook are expensive and time consuming, like Ground Vibration Testing (GVT) and flutter test. Therefore it is expected to decrease time and expenses consumed for these tests.

1.2. Objectives of the Thesis

The objective of this thesis is to determine degree of accuracy of flutter analysis results of plate like structures in incompressible flow compared to wind tunnel flutter test results and also compare the K-method and g-method solution methods of ZAERO©. It is also aimed to compare the different modal analysis results, in which different structural boundary conditions are used, with the modal test result of the plate like structure. A more accurate flutter analysis is going to decrease the number of flutter tests. This study shows the accuracy of the flutter analysis results with the wind tunnel tests for the plate like structures in incompressible flow.

In this study, flutter analysis are realized with ZAERO©, a commercial aeroelastic analysis software that uses panel method based on linearized potential flow theory. Modal parameters (natural frequencies and mode shapes) required by ZAERO© are obtained from MSC Nastran© solver. All structural FE models are constructed in MSC Patran©. Finally, all flutter tests are conducted in Ankara Wind Tunnel (ART).

1.3. Flutter

Interaction of aerodynamic, inertial and elastic forces may result in instabilities. One of the most important instability known in aeroelasticity is flutter. Flutter is an aeroelastic instability which involves bending and torsional degrees of freedom (DoF). Coupling of the torsional structural mode with a bending mode results in a flutter mode through the aerodynamic forces. Torsion of the structure is the result of the aerodynamic forces. The angle of attack is changed by the torsion. As a result of angle of attack change aerodynamic lift force is also changed [1]. The change of angle of attack due to torsion changes the lift in an unfavourable phase with the bending which results in flutter. Vibrations grow rapidly at flutter speed. Structural damping cannot compensate the negative damping caused by the flutter mode. Flutter is observed above a certain relative wind speed on the structure, this speed is called as the critical flutter speed [2].

For a cantilever wing physical phenomenon can be defined as follows: Assume there is a steady flow on the wing, and suddenly the wing is disturbed with an unsteady external load and oscillates. If the system is stable the oscillation is to be damped out when the excitation is removed. Assume the free stream velocity on the wing is increased. At a certain point damping rapidly decreases. After that point, small disturbance on the wing results an uncontrollable oscillation. Such instability is called flutter.

Forces on the body depend on the flow direction, geometry of the body, position of the body relative to flow direction and shape changes of the body in an aeroelastic phenomenon. Shape of the body and direction change and position of the body relative to the flow also depends on the forces on the body. These interactions may result in an unstable behaviour. This unstable behaviour is related to dynamic pressure and physical properties of the elastic body such as modulus of elasticity, Poisson’s ratio, and the dimensions of the body.

Since flutter is a very catastrophic failure, flutter analysis is very important especially for high speed aircrafts, space vehicles, rockets and missiles.

1.4. Historical Overview

The study of flutter begins with the research of Lanchester [3], Bairstow and Fage [4] in 1916 about the antisymmetrical flutter of a Handley Page bomber. In 1918 Blasius [5] started to make some calculations for the Albatros D3 biplane due to the failure of the lower wing. The development of the flutter analysis is increased after the development of non-stationary airfoil theory by Kutta and Joukowsky. The torsion flutter was first found by Glauret in 1929, which is discussed in detail by Smilg [6]. Several types of single degree of freedom flutter involving control surfaces at both subsonic and supersonic speeds have been found by Cheilik and Runyan [7, 8]. Pure bending flutter of a cantilever swept wing occurs if the wing is heavier than the surrounding air and has a sufficiently large sweep angle [9]. The bending torsion in an incompressible fluid has been studied by J.H.Greidanus [10]. Dugundji [11] searched for panel flutter and the rate of damping. Dowell [12, 13] investigated the two and three dimensional plate undergoing cyclic oscillations and aeroelastic instability. Cantilever beam with tip loads having an arbitrary cross section is discussed by Kosmatka [14] using a power series solution technique for the out of plane flexure and torsion case.

Subsonic flight and supersonic flight is an ordinary event nowadays. Hypersonic flights become more and more popular due to increased needs. As a result, aeroelastic analysis become more important part of the design of a new aircraft or an external store for an existing aircraft.

1.5. Literature Review

Libo et all [15] designed a wind tunnel test model for the flutter analysis. The model was used in a complete flutter certification procedure. GVT, model updating and flutter analysis were all done for this model. P-k solution method was used in flutter analysis.

Neal et all [16] worked on the design and wind tunnel analysis of a fully adaptive aircraft configuration. The goal of the study was to determine the effect of the sweep, span extension and tail extension on the aerodynamic characteristics of the model.

Omar and Kurban [17] designed a free wing unmanned aerial vehicle model and tested it in low speed closed circuit wind tunnel to see the effect of the angle of attack and Reynold's number.

Samikkannu [18] studied the details of fabrication, ground and wind tunnel testing of a scaled aeroelastic model of T-Tail with a flexible fuselage. Composite materials were used to obtain the required dynamics for the model during the GVT. Wind tunnel test was done in order to see the flutter characteristics of the model.

Strand and Levinsky [19] conducted wind tunnel tests for a free-wing tilt-propeller V/STOL airplane model in order to see aerodynamic characteristics of the model airplane. Lift and drag curves of the airplane have been obtained as a function of propeller tilt angle and thrust coefficient.

1.6. Flutter Certification Procedures

Flutter is not a well-known phenomena at the earlier times of the aviation industry. Aircrafts are flown to their maximum speeds to show that they are structurally safe at maximum speeds. After the investigation of the flutter phenomena, flutter tests became an important part of the design and modification of the air vehicles.

Figure 1 emphasizes the verification and validation steps for an aeroelastic aircraft models. As it can be seen in that figure, flutter certification is a very complicated task. Every step of this certification procedure requires a large amount of work power, time and money.

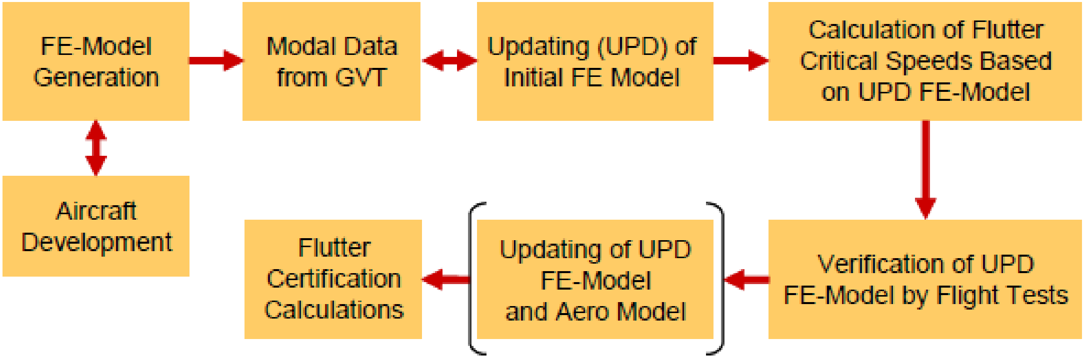

Figure 1. Actual verification and validation process of aeroelastic aircraft models [20]

TÜBİTAK-SAGE is an institute that designs external stores for the existing fighter aircrafts. Due to the addition of a new external store to the aircraft, it is necessary to show that the aircraft is free of flutter by flutter tests. Flutter certification procedure that is followed by TÜBİTAK-SAGE can be summarized as follows,

- Determination of the test configurations.
- Ground vibration testing.
- FE-model updating.
- Aeroelastic flutter analysis.
- Flight flutter tests.

1.6.1. Determination of the Test Configurations

Passenger planes do not carry external stores on them, due to this reason their flutter certification is done only once. However, fighter aircrafts are capable of carrying different type and number of external stores. Those external stores are not utilized arbitrarily. They are used in a concept of operation for the aircraft. The concept of operation defines the types and number of munitions that the combat aircraft carries and the location of the munitions on the aircraft stores. All types of store combinations are indicated clearly in the concept of operation document. All different external store configurations have their own structural and aerodynamic identity. Therefore, for each of those configurations, it is necessary to re-arrange the flutter certification procedure. Determination of the test configurations is very critical since it is the starting point of the flutter test procedure.

1.6.2. Ground Vibration Testing (GVT)

After the test configurations are determined, GVT for each configurations is conducted. GVT is necessary to validate and update the mathematical model of the aircraft by using experimentally determined low-frequency modes of the whole aircraft structure. This mathematical model of the aircraft is used in flutter analysis for reliable flutter estimations. In GVT, the aircraft is equipped with hundreds of accelerometers in order to obtain enough resolution of the motions of all structural parts of the aircraft. Several numbers of large exciters are used in order to excite the all modes in the interested frequency range of the aircraft with sufficient energy. The result of this test is used to verify and validate the finite element (FE) model of the aircraft and therefore it should be of high quality and accuracy. Test results are also used in the certification process due to the regulations of the Airworthiness Authoroties [19]. GVT may take long times. The main reason for long testing period is that the aircraft has many different configurations to be tested as mentioned before. Another reason is the organization of a test team. It used to be longer in the past to conduct a GVT. Advances in technology and science results in a dramatic decrease of the time spent for those tests. However, more complex aircraft designs and common usage of composite materials results in more complex structures. These structures result in newly developed difficulties for the GVT.

1.6.3. FE-Model Updating

After the development of the aircraft, it is necessary to develop a FE-model of the aircraft based on FEM modelling. Knowledge of the experienced workers, and experiences gained from the former development processes of similar structures are important to shorten the FE-model development time. Structural dynamic characteristics of the aircraft are obtained by performing GVT on different configurations of the aircraft. The obtained modal data provide the basis for the verification and validation process of the initial analytical model.

The results of the GVT are used for FE-model updating. Validated FE-model is used to predict the critical flutter speeds of the aircraft, then it is necessary to progress carefully in model updating stage. Due to this reason model updating procedure takes up to several weeks. Another reason for model updating to be done as accurate as possible is that the usage of the updated FE-model for the flutter calculations enables to cover future modifications on the aircraft without any additional GVT. FE-model can be updated for smaller modifications on the structure and it can be used for the flutter calculations of the modified aircraft.

1.6.4. Flutter Analysis

Updated FE-model is used in aeroelastic analysis in order to obtain an information about the flutter behaviour of the aircraft. Computer programs specialized for the flutter analysis, e.g. ZAERO©, or some finite element analysis programs such as NASTRAN©, can be used for flutter analysis. These results determine the safety limit for the flight flutter tests.

1.6.5. Flight Flutter Test

Flutter flight tests are the final step of the flutter certification procedure of the aircraft. As a result of the aeroelastic analysis, most critical configurations in terms of flutter are determined. Flight flutter tests are conducted for those critical configurations. As a result of flight flutter test, flight envelope of the aircraft is determined.

Structural excitation during the flutter test is necessary to detect the impending aeroelastic instabilities. For aircrafts, -up to 60 Hz- excitation is necessary to excite the selected vibration modes. Lower excitation results in lower aerodynamic damping values than the actual damping levels and a large scatter in damping values from the response data. Excitation system should be light enough not to change the modal characteristics of the aircraft. The most effective way to obtain the desired excitation is to use inertia shakers. Aerodynamic force is also a simple way to obtain the excitation force. In that type of excitation, aerodynamic vanes have a small airfoil is mounted at the tip of the wing or stabilizer. Atmospheric turbulence is also used for the excitation during the flight flutter tests [21]. It is necessary to have an excitation point far away from a nodal line [22].

Response of the aircraft to an excitation should also be recorded. Then, instrumentation is another important phenomena in flight flutter testing. Accelerometers are used to obtain the response of the aircraft during the flight flutter test. The location and the number of measurement points should be chosen carefully in order to get good enough data from the measurements. Pulse code modulation (PCM) or digital telemetry is used in order to transfer the measured responses from the aircraft to the ground station. Typical characteristics of a good measurement point are that data obtained from that point should reflect the mode shapes of the aircraft [23].

1.7. Outline of the Thesis

This brief introduction chapter is followed by Chapter 2, in which theoretical background of ZAERO© is explained in detail. Modal analysis and modal test results are given in Chapter 3. Flutter analysis conducted for the study are explained in Chapter 4. Chapter 5 explains the wind tunnel flutter tests. Finally, conclusions, remarks, observations, and contributions to the literature are stated in Chapter 6.

CHAPTER 2

THEORY OF FLUTTER ANALYSIS

In this study, ZAERO©, flutter analysis software based on linearized potential flow theory and developed by ZONA© Inc., is used for aeroelastic stability analysis. This chapter is devoted to the aeroelastic theory behind this software.

2.1. Aeroelastic Stability Equations [24]

The equation of motion of an aeroelastic system can be stated as follows:

$$[M_{GG}]\{\ddot{x}(t)\} + [K_{GG}]\{x(t)\} = \{F(t)\} \tag{1.1}$$

$\{F(t)\}$ consists of two parts:

$$\{F(t)\} = \{F_a(t)\} + \{F_e(t)\} \tag{1.2}$$

Combining Equations (1.1) and (1.2) gives:

$$[M_{GG}]\{\ddot{x}(t)\} + [K_{GG}]\{x(t)\} - \{F_a(t)\} = \{F_e(t)\} \tag{1.3}$$

If $\{F_a(t)\}$ is nonlinear with respect to $\{x(t)\}$, flutter analysis is performed by a time-marching procedure solving the following equation:

$$[M_{GG}]\{\ddot{x}(t)\} + [K_{GG}]\{x(t)\} - \{F_a(t)\} = 0 \tag{1.4}$$

with initial conditions $\mathrm{x}(0)$ and $\dot{\mathrm{x}}(0)$.

Amplitude linearization assumption converts Equation 1.4 into an eigenvalue problem for flutter analysis. In this case, the aerodynamic feedback $\{F_a(t)\}$ is related to the structural deformation $\{x(t)\}$ by means of the following convolution integral:

$$\{F_a(x)\} = \int_0^t q_\infty \left[H\left(\frac{V}{L}(t-\tau)\right)\right]\{x(\tau)\}\mathrm{d}\tau \tag{1.5}$$

where:

$\left[H\left(\frac{V}{L}(t-\tau)\right)\right]$ represents the aerodynamic transfer function, and L is defined as:
$L = \frac{c}{2}$

The Laplace domain counterpart of the Equation 1.5 is simply:

$$\{F_a(x(s))\} = q_\infty \left[\bar{H}\left(\frac{sL}{V}\right)\right]\{x(s)\} \tag{1.6}$$

Equation 1.4 now can readily be transformed into the Laplace domain and results in an eigenvalue problem in terms of s given as follows:

$$\left[s^2[M_{GG}] + [K_{GG}] - q_\infty \left[\bar{H}\left(\frac{sL}{V}\right)\right]\right]\{x(s)\} = \{0\} \tag{1.7}$$

2.1.1. Modal Reduction Approach [24]

Solving Equation 1.7 directly is computationally costly since the FE model of an aircraft contains large number of DOF, since the mass and stiffness matrices are very large in size. Therefore, modal reduction approach is used to solve this problem.
Structural deformation is expressed in terms of modal coordinates as follows:

$$\{\mathrm{x(s)}\} = [\Phi]\{\mathrm{q(s)}\} \tag{1.8}$$

Substituting Equation 1.8 into Equation 1.7 and pre-multiplying Equation 1.7 with $[\Phi]^T$ yields the following flutter equation:

$$\left[\mathrm{s}^2[\Phi]^T[M_{GG}][\Phi] + [\Phi]^T[K_{GG}][\Phi] - q_\infty[\Phi]^T\left[\bar{H}\left(\frac{sL}{V}\right)\right][\Phi]\right]\{\mathrm{q(s)}\}=\{0\} \tag{1.9}$$

Equation 1.9 can be written as follows:

$$\left[\mathrm{s}^2[M_{HH}] + [K_{HH}] - q_\infty\left[Q_{hh}\left(\frac{sL}{V}\right)\right]\right]\{\mathrm{q(s)}\}=\{0\} \tag{1.10}$$

where:

$[M_{HH}] = [\Phi]^T [M_{GG}][\Phi]$,

$[K] = [\Phi]^T [K_{GG}][\Phi]$,

$\left[Q_{hh}\left(\frac{sL}{V}\right)\right] = [\Phi]^T \left[\bar{H}\left(\frac{sL}{V}\right)\right][\Phi]$ is the generalized aerodynamic force matrix.

The modal reduction approach reduces the size of the eigenvalue problem. Solving this equation is easier than that of Equation 1.7. Equation 1.10 is the classical flutter matrix equation.

In order to achieve a conversion, in which the nonlinear flutter equation is converted to the classical flutter matrix equation, it is desired to obtain an aerodynamic transfer function. ZAERO© obtains unsteady aerodynamics methods in the frequency domain by assuming simple harmonic motion. Obtained aerodynamic transfer function is called the Aerodynamic Influence Coefficient (AIC) Matrix.

2.1.2. Unified *AIC* of ZAERO© [24]

ZONA6, ZONA7 are unsteady aerodynamics methods incorporated in ZAERO©, ZONA6 generates AIC matrices for subsonic flow regimes; ZONA7 generates AIC matrices for supersonic flow regimes.

One of the fundamental aerodynamic parameter is the reduced frequency and it is defined as:

$$k = \frac{\omega L}{V} \tag{1.11}$$

ZAERO© uses the panel method which is based on the linearized potential flow theory to solve the integral equations. Figure 2 shows the panel model of F-16 aircraft, each of these panels are called the aerodynamic box.

Each aerodynamic box contains a control point in which boundary conditions are applied. Addition of integrals of each box one by one gives the integral equation of the whole configuration. AIC matrix is obtained by the assembly of the elementary integral solutions and relates the structural deformation and the aerodynamic forces as follows:

$$\{F_h\} = q_\infty[AIC(ik)]\{h\} \tag{1.12}$$

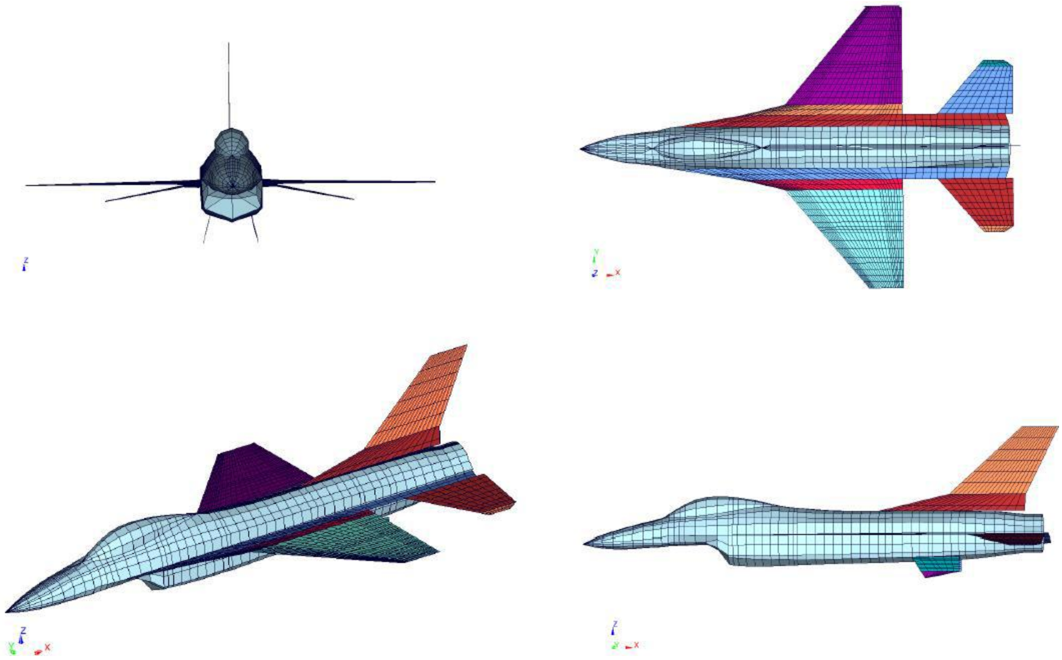

Figure 2. Panel model of F-16 aircraft [24]

For Equation 1.12 it can be said that:

- AIC matrix is computed in the reduced frequency domain (k-domain).
- AIC matrix is computed by using the panel model. Due to this fact a problem of the displacement and force transfer between the panel model and structural model occurs. This problem is solved by the spline matrix which interpolates the displacements at structural finite element grid points to aerodynamic panel model grid points.

2.1.3. Functionality of the Spline Matrix [24]

Beam spline method, infinite plate spline method, thin-plate spline method and rigid-body attachment method are used. Spline module generates a spline matrix given as:

$$\{h\} = [G]\{x\} \tag{1.13}$$

where $\{h\}$ is the displacement of the aerodynamic control points and $\{x\}$ is the displacement of the structural FE grid points.

Spline matrix [G] is used for the force transferal from the aerodynamic control points to the structural grid points by using the following equation:

$$\{F_a\} = [G]^T\{F_h\} \tag{1.14}$$

The forces at aerodynamic boxes $\{F_h\}$ and their structural equivalent values $\{F_a\}$ must do the same virtual work in their respective displacements as shown below:

$$\{\delta h\}^T\{F_h\} = \{\delta x\}^T\{F_a\} \tag{1.15}$$

Substituting Equation 1.13 into the left hand side of Equation 1.15 gives:

$$\{\delta x\}^T(\{F_a\} - [G]^T\{F_h\}) = \{0\} \tag{1.16}$$

Combining Equations 1.12 and 1.13 and substituting the resultant equation into Equation 1.14 yields:

$$\{F_a\} = q_\infty[G]^T[AIC(ik)][G]\{x\} \tag{1.17}$$

Applying the modal reduction approach yields:

$$\{Q(ik)\} = [\Phi]^T[\mathrm{G}]^T[AIC(ik)][G][\Phi] \tag{1.18}$$

2.1.4. Flutter Solution Techniques [24]

2.1.4.1. K-method [20]

The classical flutter matrix equation derived in Section 1.5.2. is given as:

$$\left[s^2[M_{hh}] + [K_{hh}] - q_\infty \left[Q_{hh}\left(\frac{sL}{V}\right)\right]\right]\{q(s)\} = \{0\} \tag{1.19}$$

Unsteady aerodynamics methods are used by ZAERO© to formulate aerodynamic transfer function in frequency domain (k-domain).

$$[\bar{H}(ik)] = [G]^T[AIC(ik)][G] \tag{1.20}$$

The frequency domain counterpart of the classical flutter matrix equation can be obtained as follows:

$$\left[-\omega^2[M_{hh}] + [K_{hh}] - q_\infty[Q_{hh}(ik)]\right]\{q\} = \{0\} \tag{1.21}$$

If we add an artificial structural damping to Equation 1.21, the K-method flutter equation is obtained as follows:

$$\left[-\omega^2[M_{hh}] + (1 + ig_s)[K_{hh}] - q_\infty[Q_{hh}(ik)]\right]\{q_{ik}\} = \{0\} \tag{1.22}$$

g_s is the added artificial structural damping.

2.1.4.2. P-K Method [24]

In order to obtain aeroelastic characteristics it is sometimes necessary to predict the damping ratio. The damping ratio is used in flight flutter tests as an indicator. P-K method is used to predict damping ratio.

Laplace domain generalized aerodynamic forces matrix is replaced to $\left[Q_{hh}\left(\frac{sL}{V}\right)\right]$ by $Q_{hh}(ik)$ and it further defines a non-dimensional Laplace parameter such that:

$$p = \frac{sL}{V} = (\gamma k + ik) \tag{1.23}$$

In P-K method, Equation 1.19 is converted to Equation 1.24 using Equation 1.23 as follows:

$$\left[\frac{V^2}{L^2}[M_{hh}]p^2 + [K_{hh}] - q_\infty[Q_{hh}(ik)]\right]\{q\} = \{0\} \tag{1.24}$$

2.1.4.3. g-method [24]

Assume an analytic function in the form of $[Q_{hh}(p)] = [Q_{hh}(g + ik)]$ in the domain of $g \geq 0$ and $g < 0$. $[Q_{hh}(p)]$ can be expanded along the imaginary axis (i.e. $g = 0$) for small g by means of damping perturbation method:

$$[Q_{hh}(p)] \approx [Q_{hh}(ik)] + g \left.\frac{\partial[Q_{hh}(p)]}{\partial g}\right|_{g=0} \qquad \text{for } g \ll 1 \tag{1.25}$$

If $[Q_{hh}(p)]$ is analytic, it must satisfy the Cauchy-Riemann equations such that:

$$\frac{\partial[Re(Q_{hh}(p))]}{\partial g} = \frac{\partial[Im(Q_{hh}(p))]}{\partial k} \tag{1.26}$$

$$\frac{\partial[Im(Q_{hh}(p))]}{\partial g} = -\frac{\partial[Re(Q_{hh}(p))]}{\partial k} \tag{1.27}$$

Combining Equations 1.26 and 1.27 yields the following general equation:

$$\frac{\partial[(Q_{hh}(p))]}{\partial g} = \frac{\partial[(Q_{hh}(p))]}{\partial(ik)} \tag{1.28}$$

Thus the term $\left.\frac{\partial[Q_{hh}(p)]}{\partial g}\right|_{g=0}$ can be replaced by:

$$\left.\frac{\partial[Q_{hh}(p)]}{\partial g}\right|_{g=0} = \left.\frac{\partial[Q_{hh}(p)]}{\partial(ik)}\right|_{g=0} = \frac{dQ_{hh}(ik)}{d(ik)} = [Q'_{hh}(ik)] \tag{1.29}$$

Substituting Equation 1.29 into Equation 1.25 yields the approximated p-domain solution of $[Q_{hh}(p)]$ in terms of k for small g:

$$[Q_{hh}(p)] \approx [Q_{hh}(ik)] + g[Q'_{hh}(ik)] \tag{1.30}$$

Substituting Equation 1.30 into 1.19 yields the g-method equation as follows:

$$\left[\frac{V^2}{L^2}[M_{hh}]p^2 + [K_{hh}] - q_\infty[Q'_{hh}(ik)]g - q_\infty[Q_{hh}(ik)]\right]\{q\} = \{0\} \tag{1.31}$$

CHAPTER 3

MODAL ANALYSIS AND EXPERIMENTS

3.1. Test Configurations

Within the scope of this thesis, two different plate like structures have been analyzed and tested for flutter. First structure is a rectangular polycarbonate (PC) plate dimensions of which is 5x125x1000 mm. The second structure is a 1/10 scaled F-16 wing like PC plate which has 5 mm thickness and which is capable of carrying external stores on it. Dimensions of the second test item are given in Figure 3. Six different cylindrical shaped external stores are used during flutter tests. Store dimensions are given in Table 1. The main reason of manufacturing plate like structures from PC is to save the ART from serious damages that may be caused by breaking of the plate due to flutter. Material properties of PC obtained from literature are used in FE model of the plate structures are given in Table 2.

Table 1. Store configurations used in 1/10 scaled F-16 wing like plate

Store #	Material	Diameter [mm]	Length [mm]
1	Aluminum	10	363
2	Aluminum	20	363
3	Aluminum	40	363
4	Steel	10	363
5	Steel	20	363
6	Steel	40	363

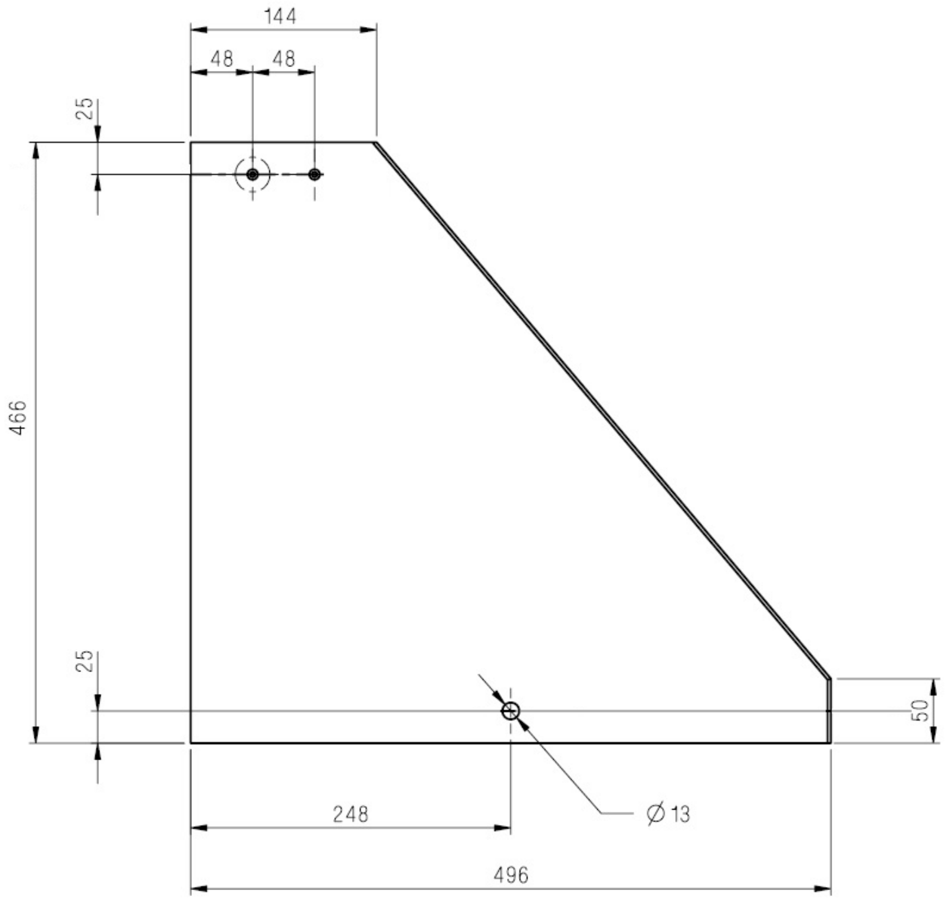

Figure 3. Dimensions of 1/10 Scaled F-16 Wing Like Plate

Table 2. Material properties of PC used in FE model

Property	Value
Elastic Modulus [MPa]	2.5
Poisson Ratio	0.35
Density [kg/m^3]	1.2

3.2. FE Models

Modal analysis of the plate like structures are carried out by MSC. NASTRAN©. Two separate FE models are constructed for 1/10 scaled F-16 wing like plate. FE models are different from each other in terms of modelling of the fixed boundary condition. Modal data of the FE model that correlate best with the modal test data is used in flutter analysis.

3.2.1. FE Model of the Rectangular Plate

It is seen in Figure 4 that first four modes are first bending at 1.08 Hz, second bending at 6.75 Hz, first torsion at 14.89 Hz and third bending at 18.90 Hz in sequence for the rectangular plate. First 10 natural frequencies are also given in Table 3. Plate is modelled similar to the cantilever beam. One end of the plate is kept fixed. In order to visualize the mode shapes better, deformations are exaggerated in the figures.

3.2.2. FE Model of the 1/10 Scaled F-16 Wing Like Plate

Two separate FE models are constructed for 1/10 scaled F-16 wing like plate. FE models are different from each other in terms of modelling of the fixed boundary condition. In the first FE model, only root of the plate is fixed as shown in Figure 5. In the second FE model, root of the plate with the side surfaces -same as the wind tunnel test- are fixed as shown in Figure 6. The natural frequencies of the second model are greater than the first one as expected. For the 1/10 scaled F-16 wing like plate a modal test is also done with impact hammer in order to compare the results.

First four mode shapes and natural frequencies of the 1/10 scaled F-16 wing like plate are given in Figure 7. First four mode shapes and natural frequencies of the same plate with other boundary condition are given in Figure 8.

Impact hammer modal test configurations for the wing like plate are shown in Figure 9, Figure 10 and Figure 11. Modal test is conducted by using the wind tunnel test fixture in order to achieve the same boundary condition as in the wind tunnel test.

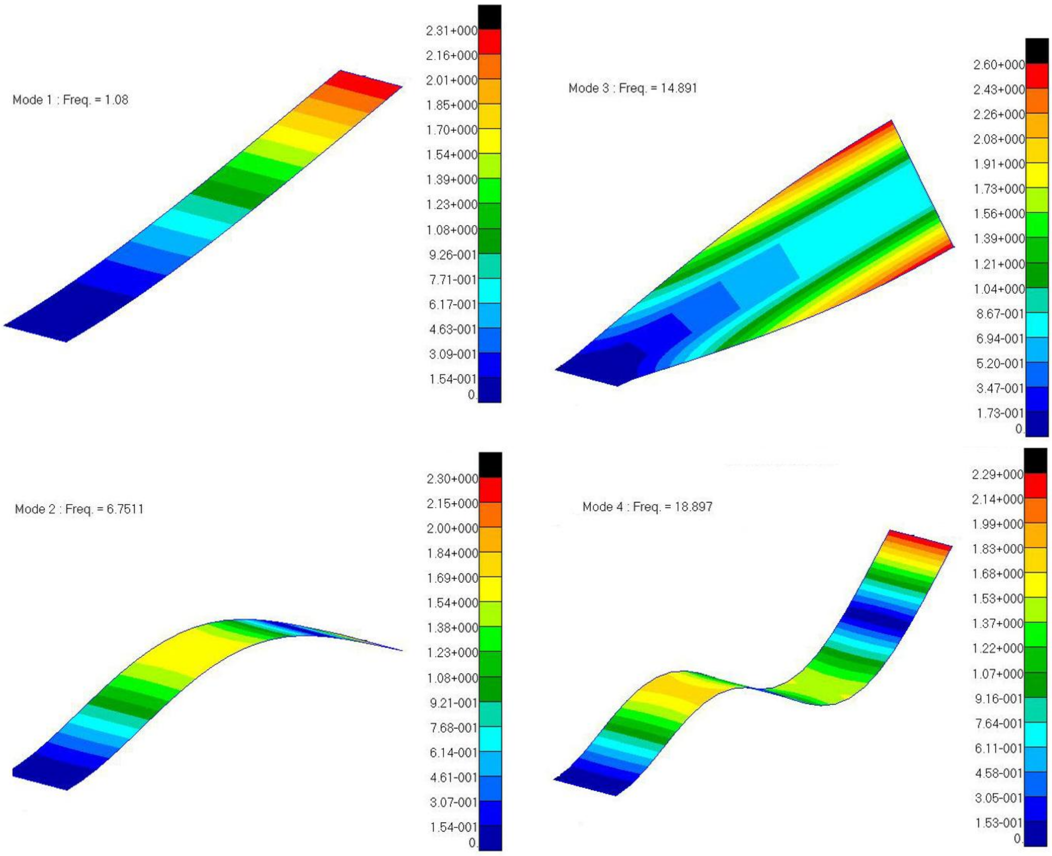

Figure 4. First four modes of the rectangular plate

Table 3. First 10 natural frequencies of the rectangular plate

Mode no	Frequency (Hz)
1	1.08
2	6.75
3	14.89
4	18.89
5	26.45
6	37.07
7	44.95
8	61.38
9	75.86
10	91.85

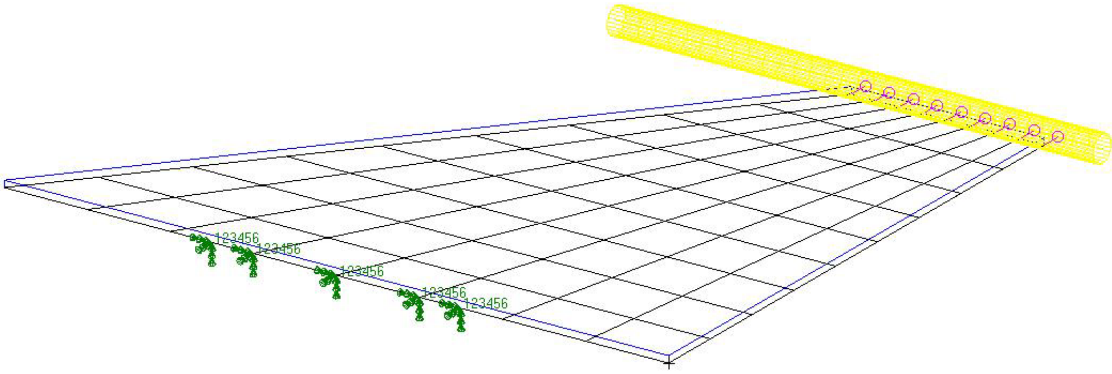

Figure 5. First boundary condition of the FE model

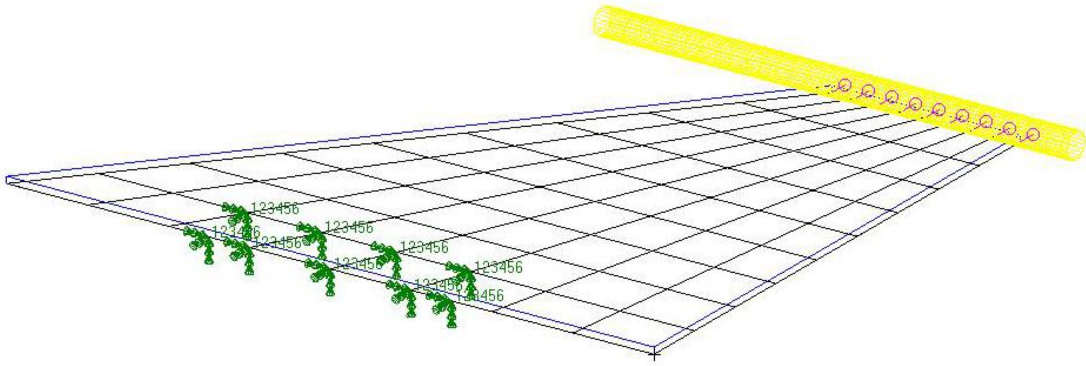

Figure 6. Second boundary condition of the FE model

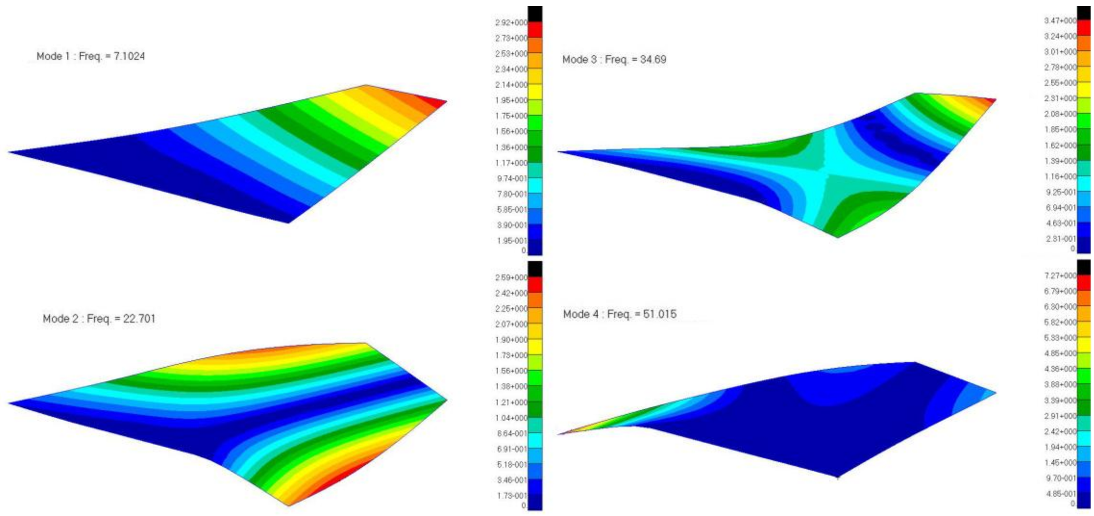

Figure 7. First four modes of the 1/10 scaled F-16 wing like plate for the first boundary condition FE model

Table 4 gives the first 10 natural frequencies of the FE model for two different boundary conditions and first 7 natural frequencies of the modal test for the 1/10 scaled F-16 wing like plate.

Comparison of the modal analysis results with the modal test results indicates that first modal analysis results are more similar to modal test results. Even the second analysis boundary condition is more realistic, the results are not in good agreement with the modal test results. Examining these results prove that flutter analysis with the first boundary condition is expected to be more realistic than the second boundary condition.

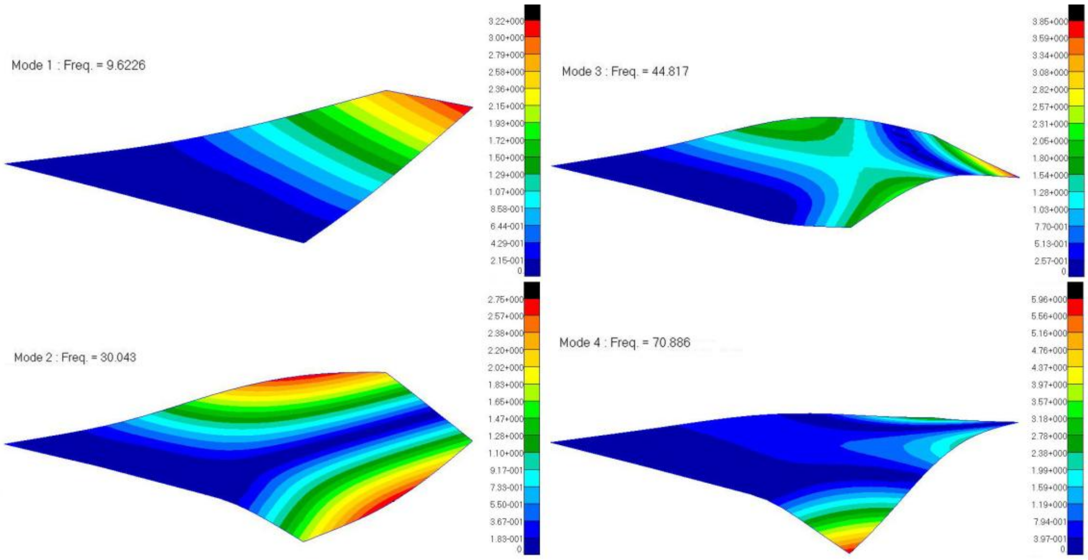

Figure 8. First four modes of the 1/10 scaled F-16 wing like plate for the second boundary condition FE model

Figure 9. Modal test configuration for the 1/10 scaled F-16 wing like plate

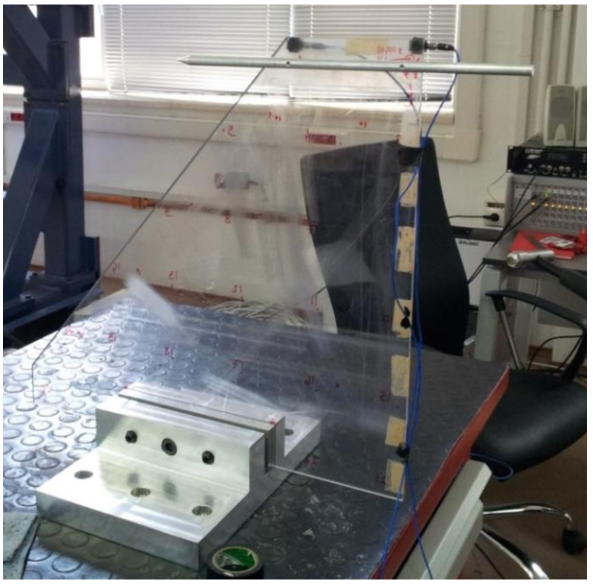

Figure 10. Modal test confiiguration for the 1/10 scaled F-16 like plate (continued)

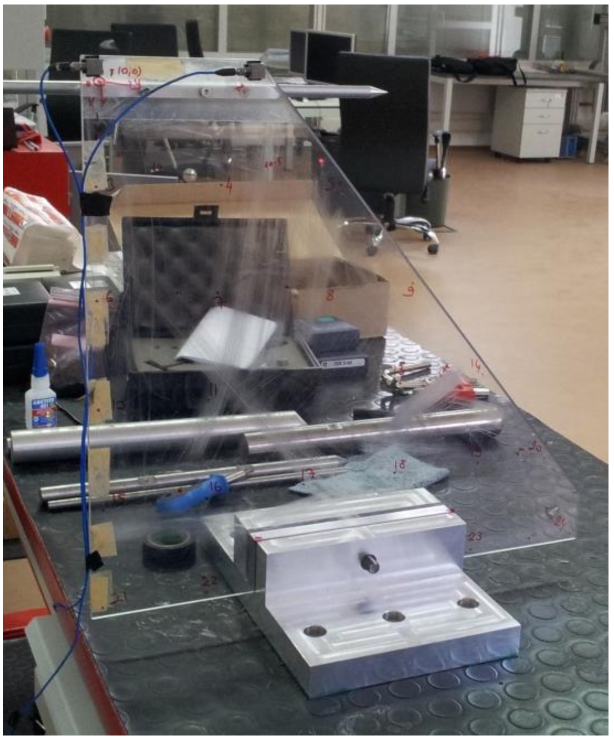

Figure 11. Modal test configuration for the 1/10 scaled F-16 like plate (continued)

Table 4. Natural frequencies of the 1/10 scaled F-16 wing like plate

Mode no	Frequency (Hz) First boundary condition	Frequency (Hz) Second boundary condition	Frequency (Hz) Modal test
1	7.1	9.62	7.06
2	22.7	30.04	24.85
3	34.69	44.82	33.66
4	51.02	70.89	57.80
5	64.44	78.16	67.80
6	77.79	88.80	99.88
7	116.3	133.98	108.19
8	124.86	139.99	-
9	150.43	159.76	-
10	190.03	201.37	-

3.2.3. FE Model of the 1/10 Scaled F-16 Wing Like Plate with External Stores

Figure 12 shows the first four natural frequencies and mode shapes for the 1/10 scaled F-16 wing like plate with a 10 mm diameter aluminum store at the wing tip for the boundary condition in which only the root of the plate is fixed. Similar results for the second analysis case are given in Figure 13. Table 5 gives the first 10 natural frequencies of the FE model for two different boundary conditions and first 8 natural frequencies of the modal test.

Results of other configurations are given in Appendix A.

Comparison of two different modal analysis results with the modal test results indicates that modal analysis results with first boundary condition are more realistic and more similar to modal test results. Then, it is expected to have more accurate flutter analysis results by using the first modal analysis results. Due to that reason, first modal analysis results are used in flutter analysis of 1/10 scaled F-16 wing like plate.

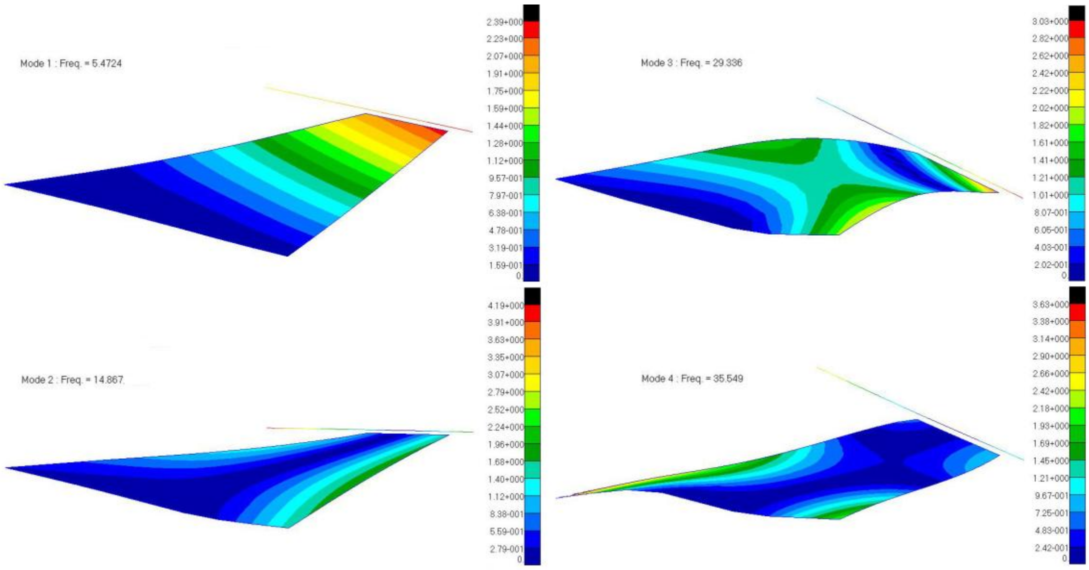

Figure 12. First four modes of the 1/10 scaled F-16 wing like plate with 10 mm diameter aluminum external store for the first boundary condition model

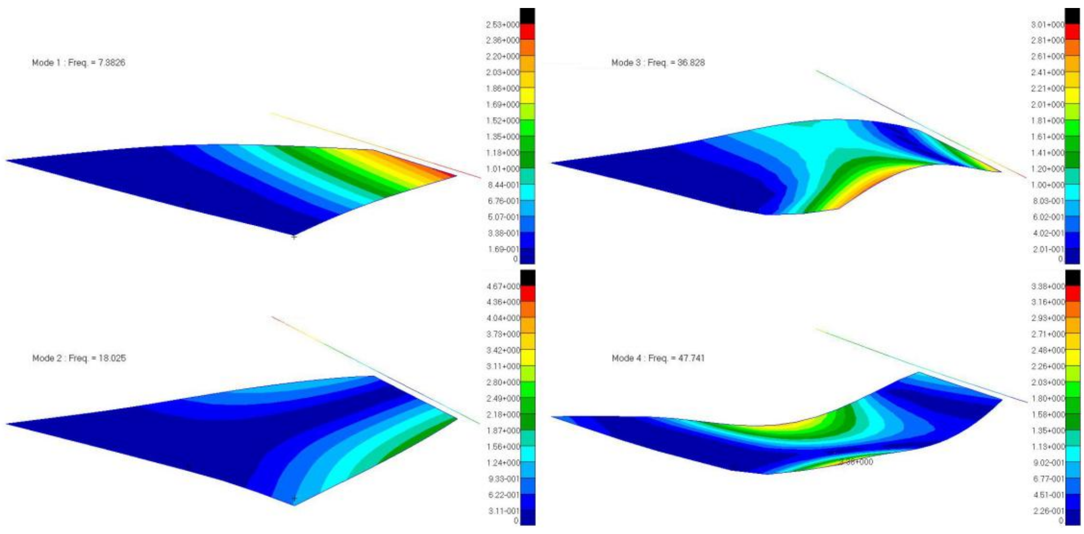

Figure 13. First four modes of the 1/10 scaled F-16 wing like plate with 10 mm diameter aluminum external store for the second boundary condition model

Table 5. Natural frequencies of the 1/10 scaled F-16 wing like plate with 10 mm diameter aluminum external store

Mode no	Frequency (Hz) First boundary condition	Frequency (Hz) Second boundary condition	Frequency (Hz) Modal test
1	5.47	7.38	5.340
2	14.87	18.03	18.97
3	29.34	36.83	30.13
4	35.55	47.74	46.24
5	43.71	70.87	58.87
6	65.05	75.57	64.14
7	91.97	109.02	92.81
8	108.71	127.34	104.01
9	132.69	134.36	-
10	136.68	151.95	-

CHAPTER 4

FLUTTER ANALYSIS

In this section flutter analysis results are given for each configuration. Aeroelastic model of the test items are prepared in ZAERO© software. The modal data obtained in the previous section is used by ZAERO© software for flutter analysis.

4.1. Flutter Analysis of the Rectangular Plate

Flutter analysis of the rectangular plate is conducted by using the FE model data. Since the test item is very simple modal test is not conducted to compare with the FE model data.

4.1.1. Aeroelastic Model

Aeroelastic model of the rectangular plate obtained with ZAERO© is shown in Figure 14. Half of the system is modelled in order to simplify the model and shorten the analysis time. The body is modelled as a cylinder and the tip of the body is sharpened in order not to affect the flow around the rectangular plate during flutter analysis.

Aeroelastic model of the rectangular plate has 40 elements in spanwise direction and 5 elements in chordwise direction. The body in the aeroelastic model has 125 mm diameter in its cylindrical section, diameter of the tip of the body changes with the x-coordinate as shown in Table 6.

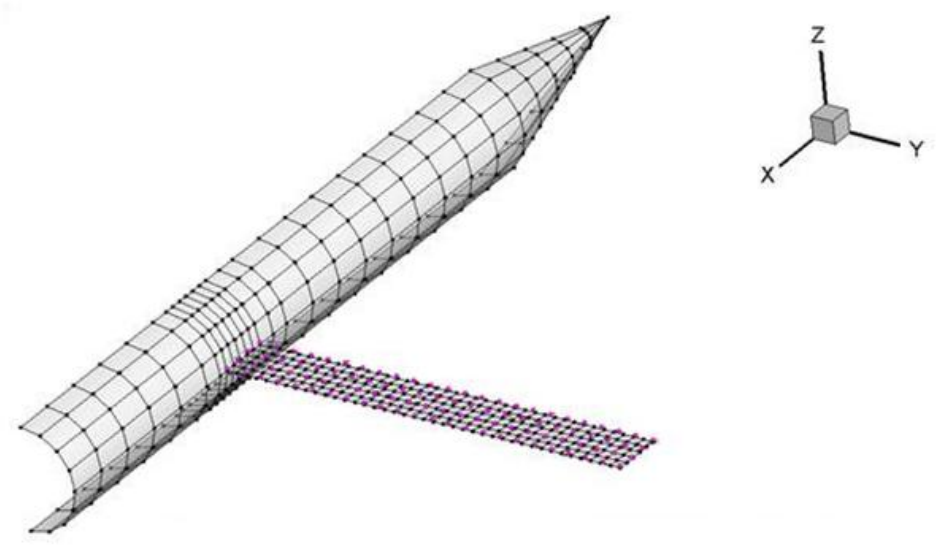

Figure 14. Aeroelastic model of the rectangular plate

Table 6. Tip diameter change of the body according to x-coordinate

x-coordinate [mm]	Diameter at that section [mm]
0	0
100	25
200	50
300	75
400	100
500	125

4.1.2. Flutter Analysis Results of the Rectangular Plate

Results of the flutter analysis for the rectangular plate indicate a flutter speed between 22.5 m/s and 23.9 m/s and a flutter frequency between 10.4 Hz and 9.7 Hz for the assumed structural damping between 0% and 4% at the third mode as shown in Table 7. Figure 15 shows the damping-speed graph (V-g plot) and Figure 16 shows the frequency-speed graph (V-f plot) of the rectangular plate for the first four modes. The V-g diagram shows that the damping of mode 3 crosses the zero damping axis at 22.5 m/s indicating a flutter boundary of the rectangular plate.

Table 7. Flutter analysis results for the rectangular plate

Structural damping [G]	0.0%	0.50%	1.0%	1.5%	2.0%	2.5%	3.0%	3.5%	4.0%
Speed [m/s] g-method	22.5	22.6	22.8	23.0	23.2	23.3	23.5	23.7	23.9
Frequency [Hz] g-method	10.4	10.3	10.2	10.2	10.1	10.0	9.9	9.8	9.7
Speed [m/s] K-method	23.8	24.0	24.2	24.4	24.6	24.8	25.0	25.2	25.4
Frequency [Hz] K-method	9.7	9.6	9.5	9.4	9.3	9.2	9.1	9.0	8.9

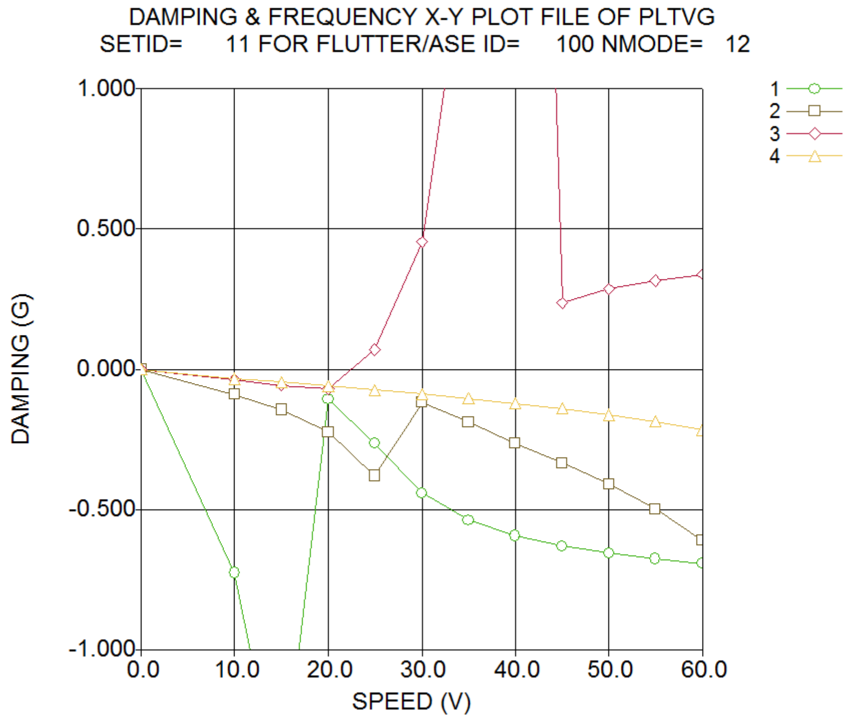

Figure 15. V-g plot of the rectangular plate

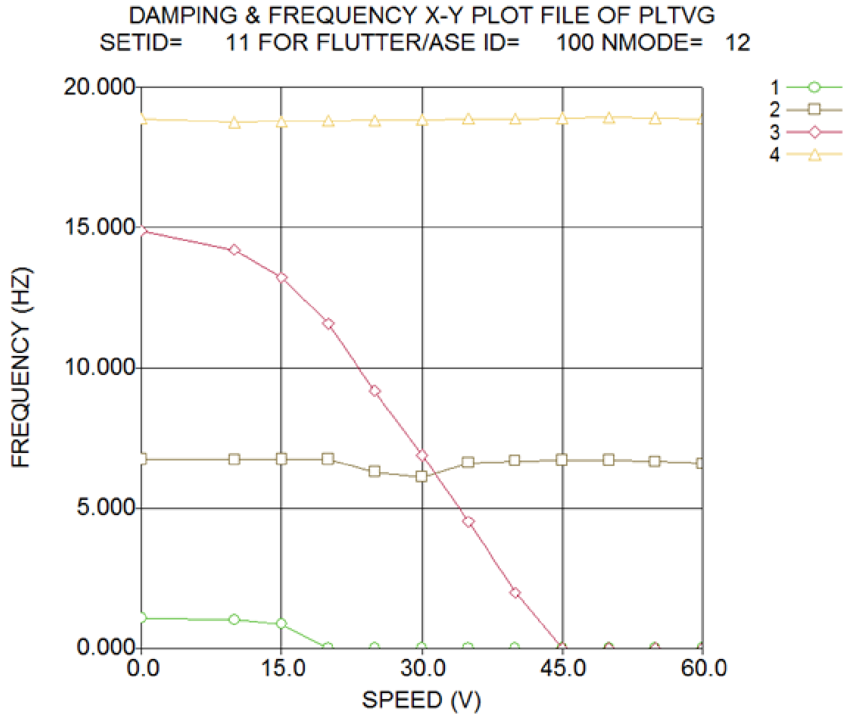

Figure 16. V-f plot of the rectangular plate

4.2. Flutter Analysis of the 1/10 scaled F-16 wing Like Plate

Flutter analysis are conducted by using two different modal analysis data. First analysis results are for the modal analysis in which only the bottom of the plate is kept fixed. Second analysis results are for the modal analysis in which the bottom and side surfaces of the plate are fixed similar to wind tunnel test fixture.

4.2.1. Aeroelastic Model

Aeroelastic model of the 1/10 scaled F-16 wing like plate is shown in Figure 17. Figure 18 shows the aeroelastic model of the same wing with a 10 mm diameter aluminum weight. Similar models are created for the other configurations, too.

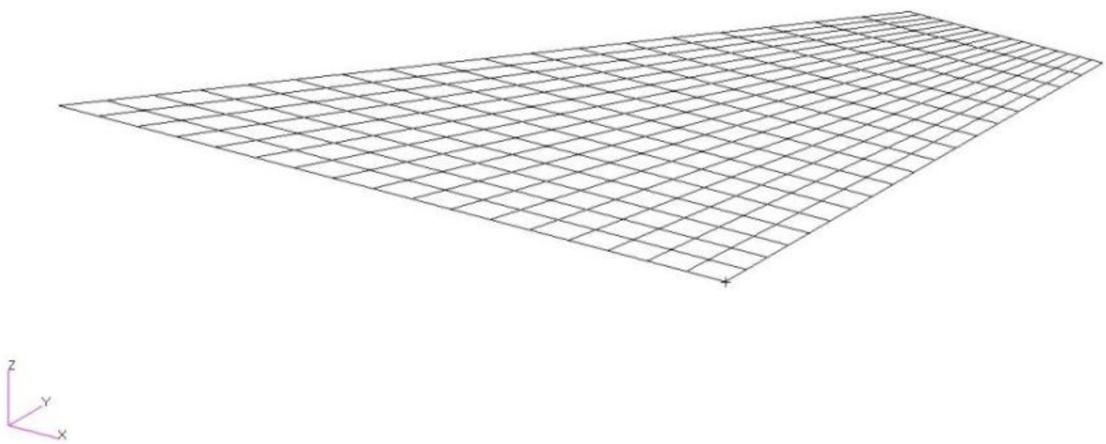

Figure 17. Aeroelastic model of the 1/10 scaled F-16 wing like plate

4.2.2. Flutter Analysis Results of the 1/10 Scaled F-16 Wing Like Plate

It is seen in modal analysis and modal test results that using first boundary condition in modal analysis of 1/10 scaled F-16 wing like plate is more similar to modal test results when compared to modal analysis with second boundary condition. Then, flutter analysis results with the first modal analysis data is expected to be more accurate. Therefore, flutter analysis results with modal data by using first boundary condition is presented in this chapter.

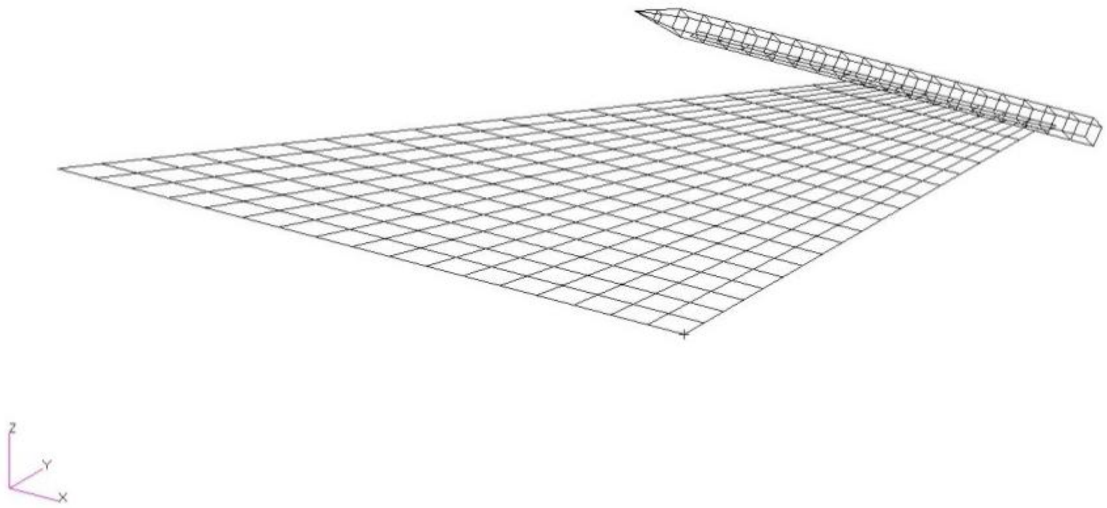

Figure 18. Aeroelastic model of the 1/10 scaled F-16 wing like plate with a 10 mm diameter aluminum store

Table 8 summarizes flutter analysis result conducted by ZAERO© for the 1/10 scaled F-16 wing like plate. Flutter speeds and flutter frequencies are given in that table obtained by the g-method and K-method solution techniques. Results are shown according to the assumed structural damping of the system up to 4%. As the structural damping of the system increases, flutter speed increases and flutter frequency decreases as expected. Results of the flutter analysis for the 1/10 scaled F-16 wing like plate indicates a flutter speed between 56.3 m/s and 57.4 m/s and a flutter frequency between 16.4 Hz and 16.0 Hz at assumed structural damping between 0% and 4% at the second mode as shown in Table 8. Figure 19 shows the V-g plot; Figure 20 shows the V-f plot of the 1/10 scaled F-16 wing like plate for the first four modes. The V-g diagram shows that the damping of mode 2 crosses the zero damping axis at 56.3 m/s indicating a flutter boundary of the 1/10 scaled F-16 wing like plate.It is also obtained from the output file that, first and second modes contribute mostly for the flutter onset.

Table 8. Flutter analysis results for the 1/10 scaled F-16 wing like plate

Structural damping [G]	0.0%	0.50%	1.0%	1.5%	2.0%	2.5%	3.0%	3.5%	4.0%
Speed [m/s] g-method	56.3	56.4	56.6	56.7	56.9	57.0	57.1	57.3	57.4
Frequency [Hz] g-method	16.4	16.3	16.3	16.3	16.2	16.2	16.1	16.1	16.0
Speed [m/s] K-method	51.0	51.2	51.4	51.6	51.8	52.1	52.3	52.5	52.7
Frequency [Hz] K-method	17.7	17.6	17.5	17.4	17.4	17.3	17.2	17.1	17.0

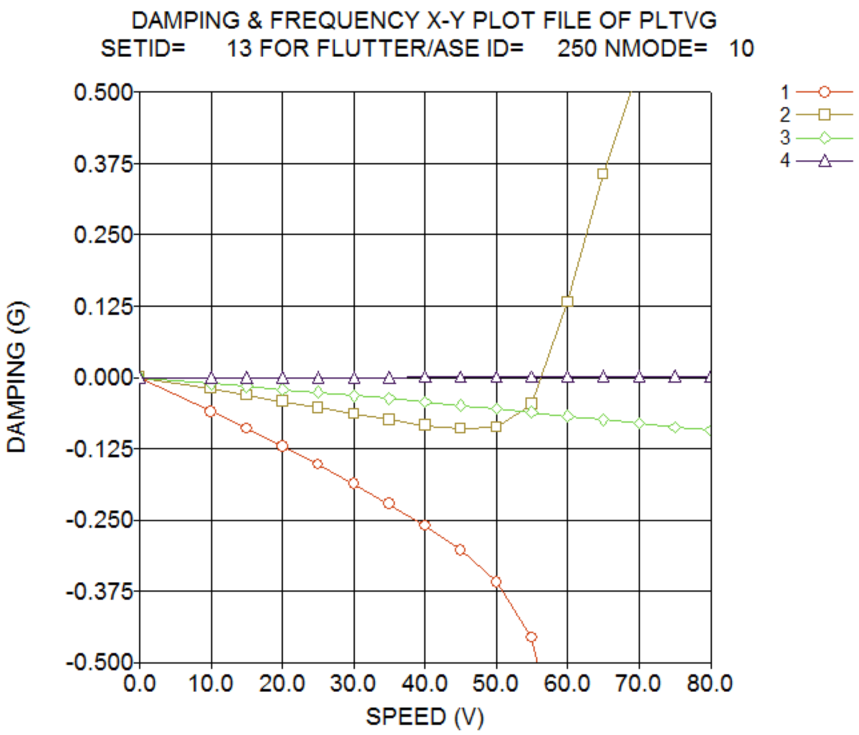

Figure 19. V-g plot of the 1/10 scaled F-16 wing like plate

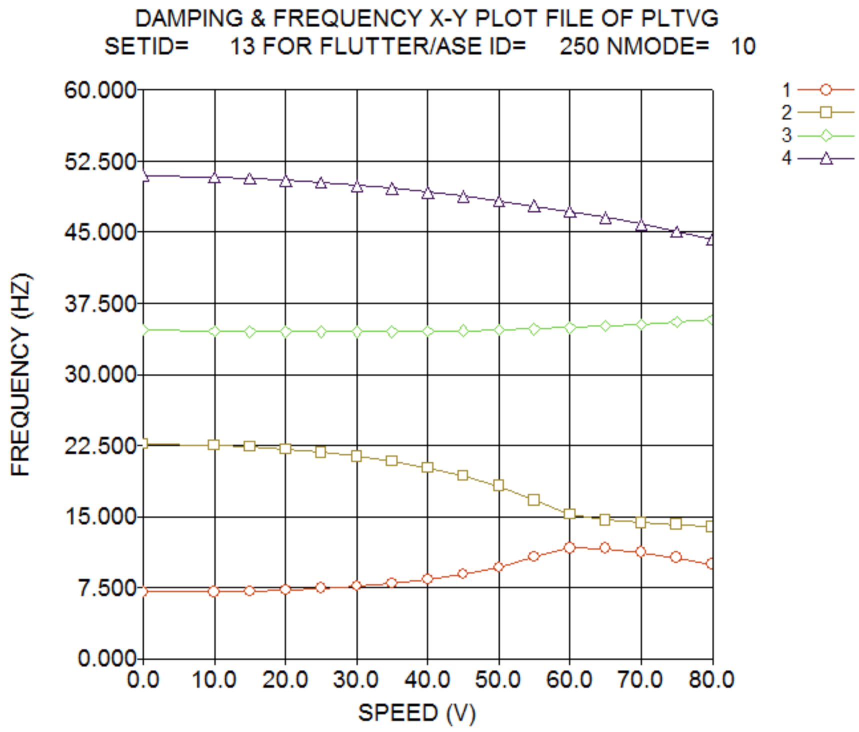

Figure 20. V-f plot of the 1/10 scaled F-16 wing like plate

Table 9 summarizes flutter analysis result conducted by ZAERO© for the 1/10 scaled F-16 wing like plate with 10 mm diameter aluminum store. Results of g-method and K-method solutions for the flutter speeds and flutter frequencies are given in that table. Results of the flutter analysis for the 1/10 scaled F-16 wing like plate with a 10 mm diameter aluminum store indicates a flutter speed between 52.7 m/s and 56.1 m/s and a flutter frequency between 11.1 Hz and 10.5 Hz at assumed structural damping between 0% and 4% at the second mode as shown in Table 9. Figure 21 shows the V-g plot; Figure 22 shows the V-f plot of the 1/10 scaled F-16 wing like plate with 10 mm diameter aluminum store for the first four modes. The V-g diagram shows that the damping of mode 2 crosses the zero damping axis at 52.7 m/s indicating a flutter boundary of 1/10 scaled F-16 wing like plate with 10 mm diameter aluminum store. It is also obtained from the output file that, first and second modes contribute mostly for the flutter onset.

Table 9. Flutter analysis results for the 1/10 scaled F-16 wing like plate with a 10 mm diameter aluminum store

Structural damping [G]	0.0%	0.50%	1.0%	1.5%	2.0%	2.5%	3.0%	3.5%	4.0%
Speed [m/s] g-method	52.7	53.7	54.8	55.7	55.8	55.9	56.0	56.1	56.1
Frequency [Hz] g-method	11.1	11.0	10.8	10.7	10.6	10.6	10.5	10.5	10.5
Speed [m/s] K-method	53.0	54.1	55.1	55.7	55.7	55.8	55.9	56.0	56.1
Frequency [Hz] K-method	11.1	10.9	10.7	10.6	10.6	10.6	10.5	10.5	10.4

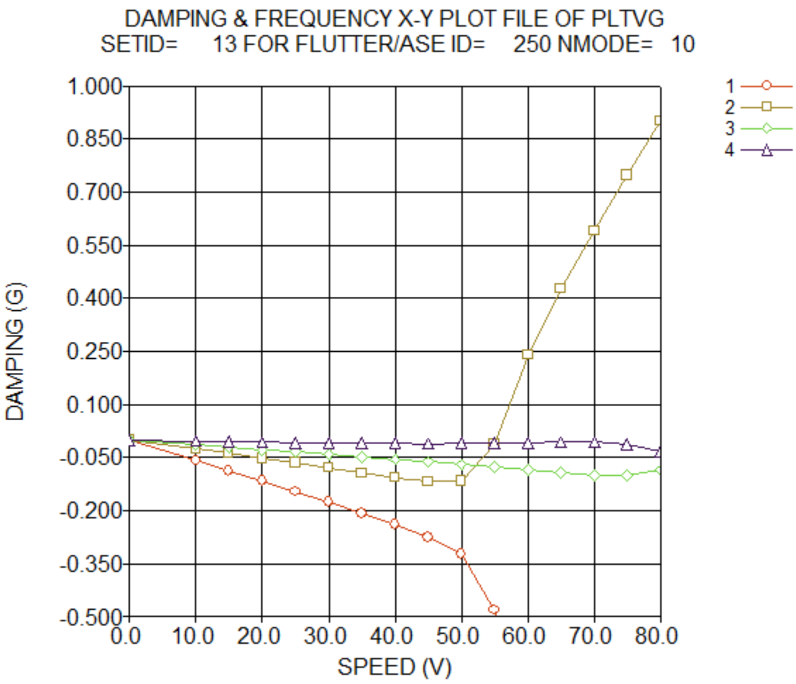

Figure 21. V-g plot of the 1/10 scaled F-16 wing like plate with a 10 mm diameter aluminum store

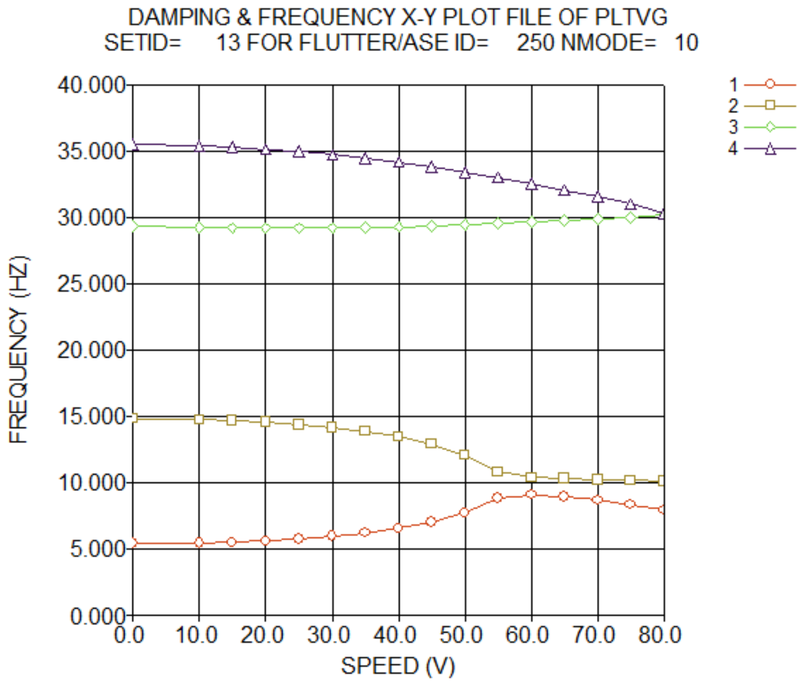

Figure 22. V-f plot of the 1/10 scaled F-16 wing like plate with a 10 mm diameter aluminum store

Similar results for other configurations are given in Appendix A. Investigation of the flutter analysis results indicates that there is a decrease in the flutter speed as the weight of the external store increases. Similarly, flutter frequency decreases as the weight of the external store increases. This trend is not valid for the 40 mm diameter stores. For those configurations, deflection of the test item is too large. That deflection may cause to ruin the flow around the plate and results in an increase in the flutter speed.

CHAPTER 5

WIND TUNNEL FLUTTER TESTS

Wind tunnel tests are conducted at Ankara Wind Tunnel (ART). ART is a subsonic wind tunnel. The wind tunnel is capable of reaching the maximum speed of 85 m/s. Wind tunnel atmospheric pressure is measured as 13.39 psi. Ambient temperature is measured as 17.1˚C.

5.1. Wind Tunnel Flutter Test of the Rectangular Plate

Firstly, wind tunnel test of the rectangular plate is conducted. Plate is fixed to the floor of the wind tunnel with a fixture as shown in Figure 23. Strain gages are used to obtain strain data and they are positioned at the root of the plate as shown in Figure 24. The strain data obtained from the strain gages during the wind tunnel test is given in Figure 25. Strain values change in an uncontrolled manner during the flutter occurrence as shown in strain-time graph. After flutter observation in test, the wind tunnel is stopped and the strain data goes back to its normal progress.

Wind tunnel speed is 24.89 m/s when the flutter is observed at the rectangular plate during the rectangular plate wind tunnel test.

5.2. Wind Tunnel Flutter Test of the 1/10 scaled F-16 wing Like Plate

In wind tunnel flutter test of the 1/10 scaled F-16 wing like plate combinations plate is again fixed to the floor of the wind tunnel with the same fixture as shown in Figure 26. In these tests acceleration data is read from the accelerometers. Accelerometers are equipped at the tip of the plate as shown in Figure 27. Acceleration-time graph for all test configurations are given between Figure 28 and Figure 34. All those figures indicate that during the flutter occurrence acceleration data increases uncontrollably and it decreases after the wind tunnel is stopped. Post-processing of acceleration data gives the flutter frequency for each configuration and those frequencies are given between Figure 35 and Figure 41.

Wind tunnel test results for the entire wing like plate combinations are summarized in Table 10. There is a tendency of flutter speed decrease as the load on the plate increases, as expected. However, this trend is not valid for the 40 mm diameter steel store configuration. It is more probably due to the fact that, plate is deflected largely and this fact resulted in an unexpected situation for this case.

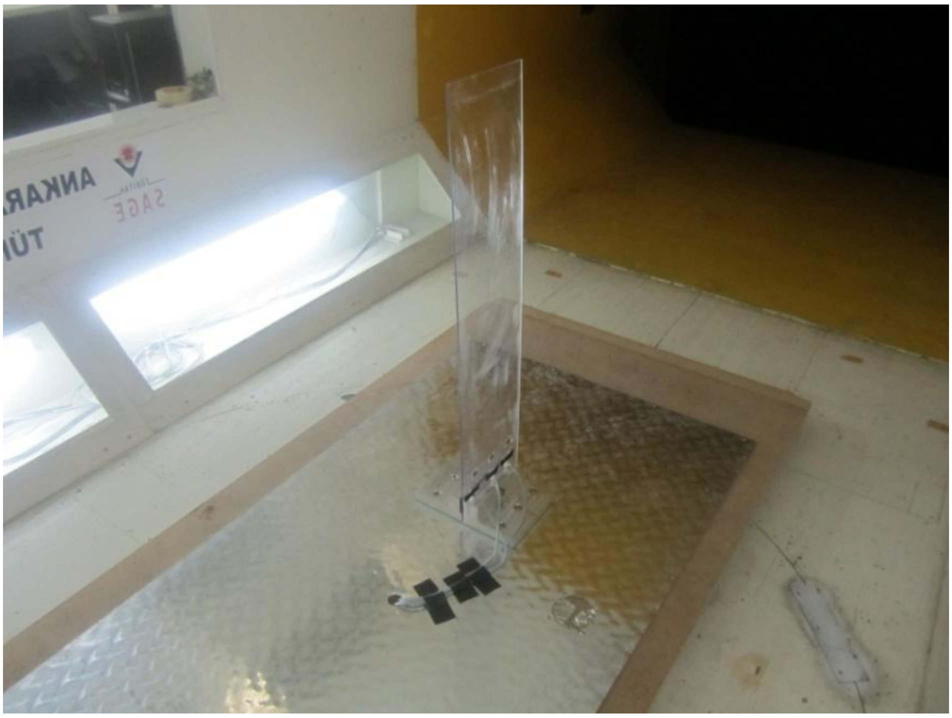

Figure 23. Wind tunnel test configuration for the rectangular plate

Figure 24. Strain gage placement for the rectangular plate test

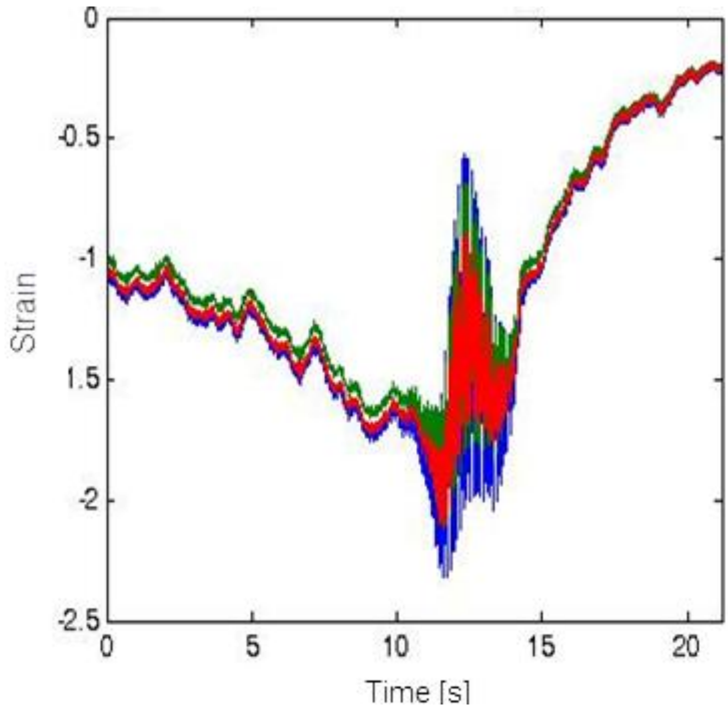

Figure 25. Strain-time graph of the rectangular plate test item during the wind tunnel test

Figure 26. Wind tunnel test configuration for the 1/10 scaled F-16 wing like plate

Figure 27. Accelerometer placement for the 1/10 scaled F-16 wing like plate in wind tunnel test

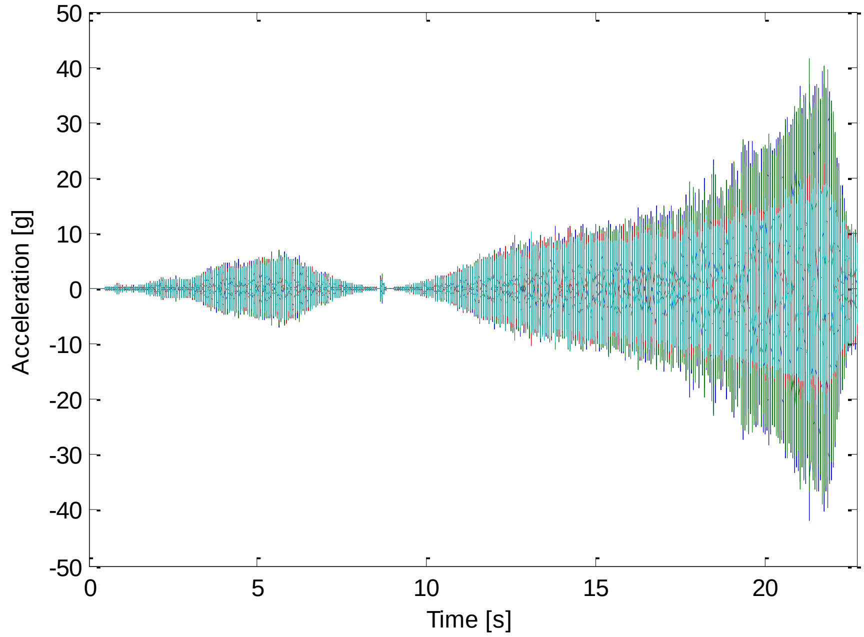

Figure 28. Acceleration-time graph for the 1/10 scaled F-16 wing like plate

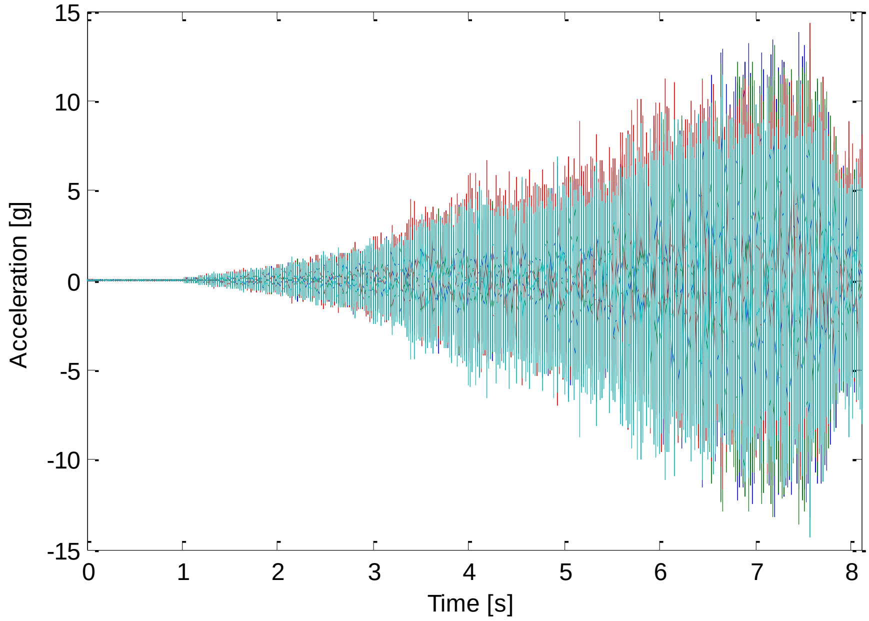

Figure 29. Acceleration-time graph for the 1/10 scaled F-16 wing like plate with 10 mm diameter aluminum store

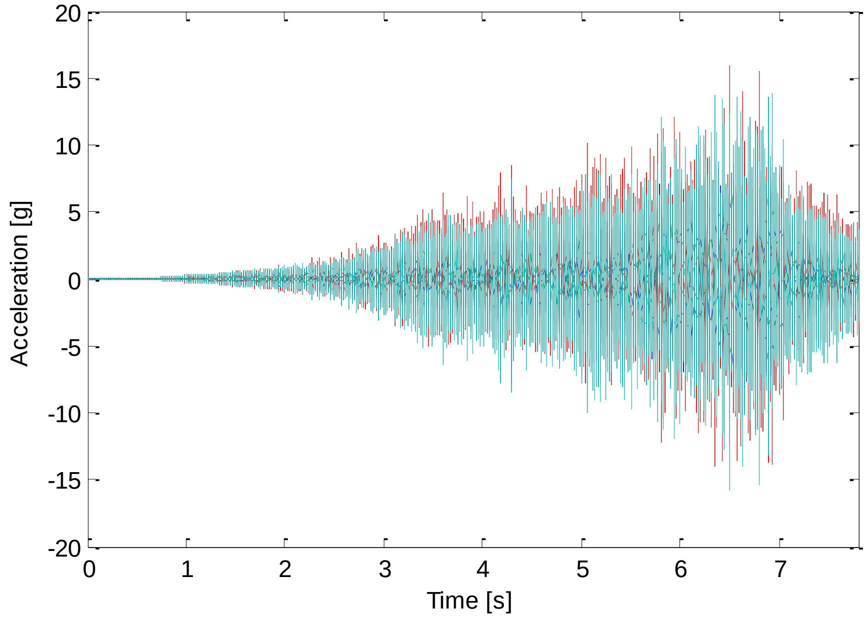

Figure 30. Acceleration-time graph for the 1/10 scaled F-16 wing like plate with 20 mm diameter aluminum store

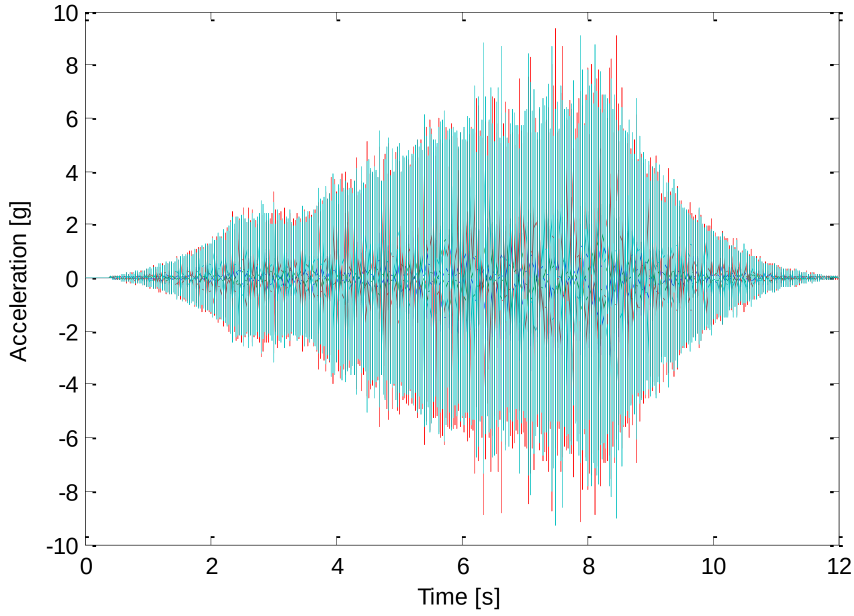

Figure 31. Acceleration-time graph for the 1/10 scaled F-16 wing like plate with 40 mm diameter aluminum store

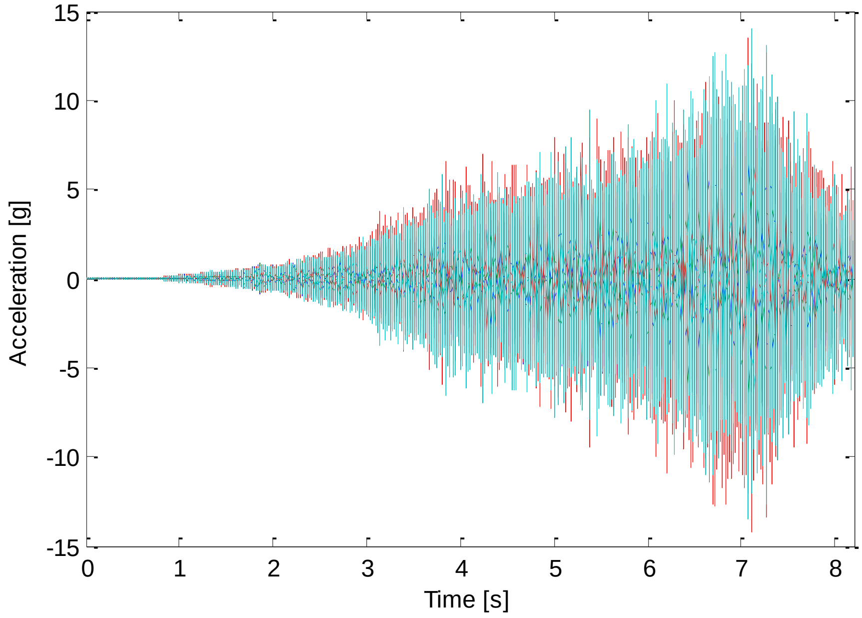

Figure 32. Acceleration-time graph for the 1/10 scaled F-16 wing like plate with 10 mm diameter steel store

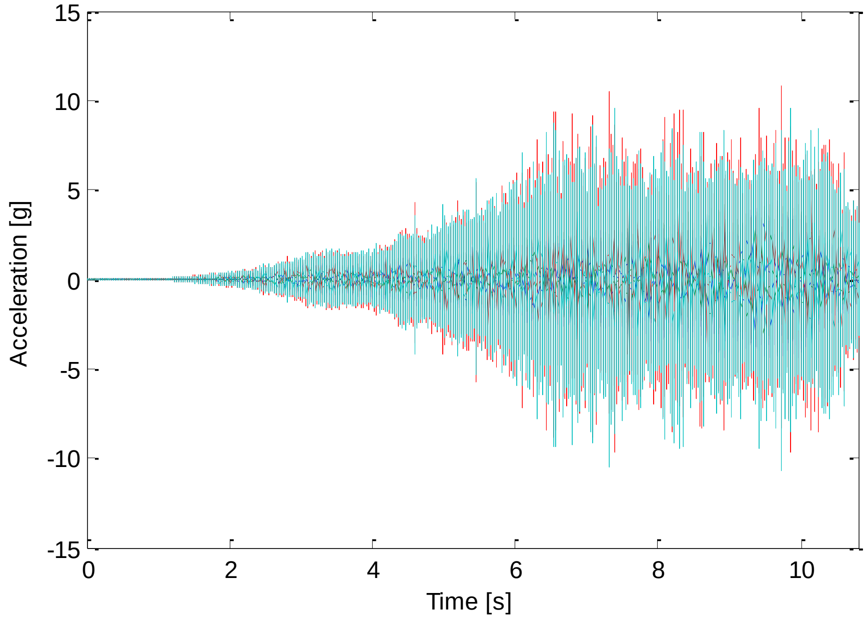

Figure 33. Acceleration-time graph for the 1/10 scaled F-16 wing like plate with 20 mm diameter steel store

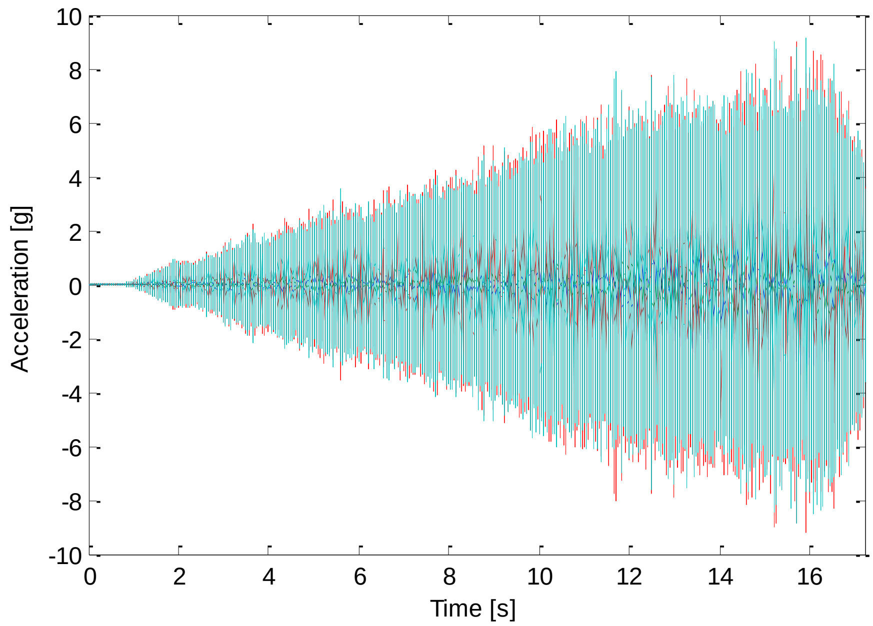

Figure 34. Acceleration-time graph for the 1/10 scaled F-16 wing like plate with 40 mm diameter steel store

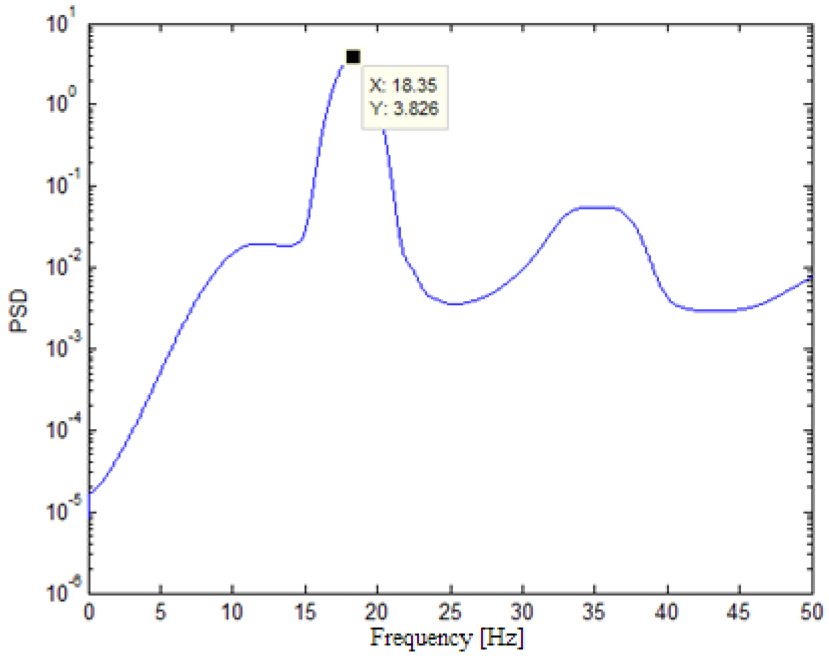

Figure 35. Flutter frequency of the 1/10 scaled F-16 wing like plate

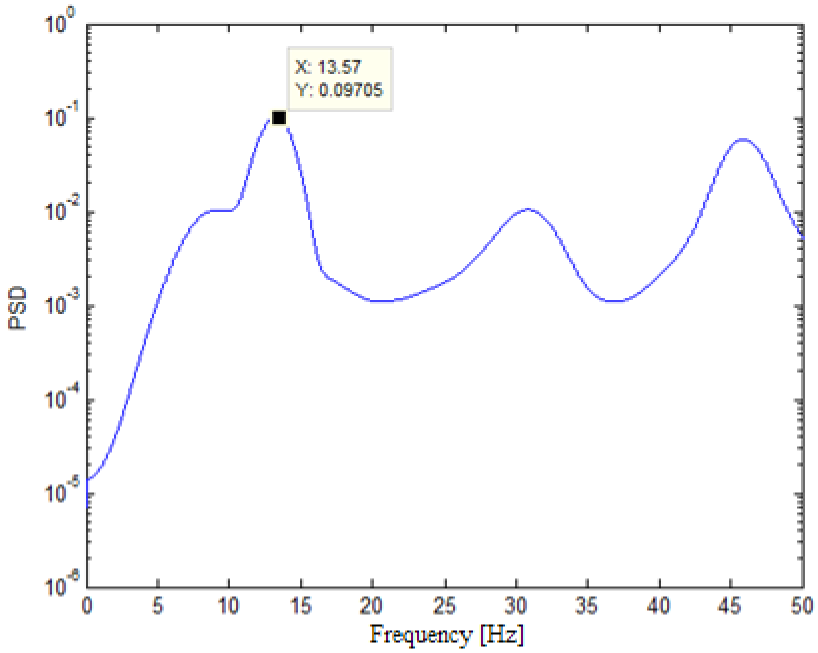

Figure 36. Flutter frequency of the 1/10 scaled F-16 wing like plate with 10 mm diameter aluminum store

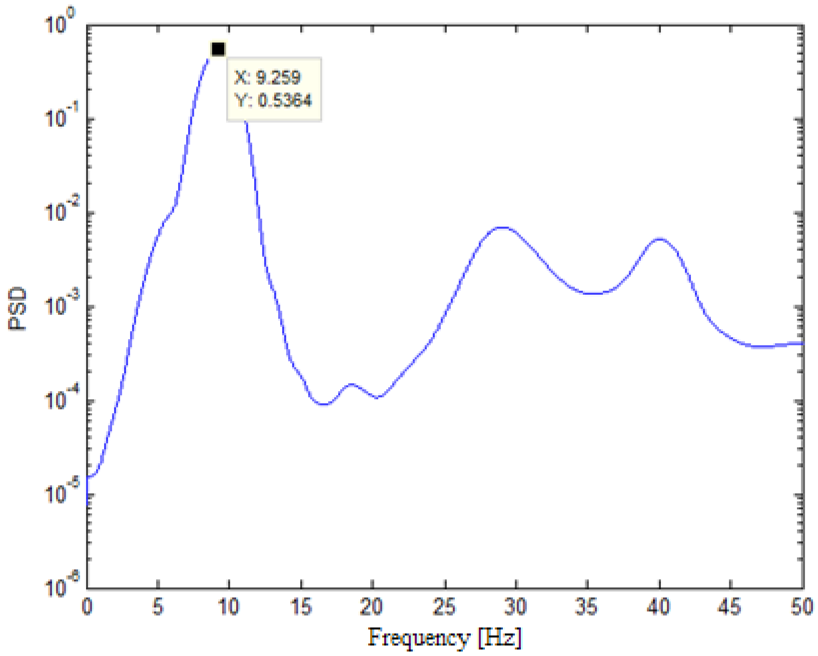

Figure 37. Flutter frequency of the 1/10 scaled F-16 wing like plate with 20 mm diameter aluminum store

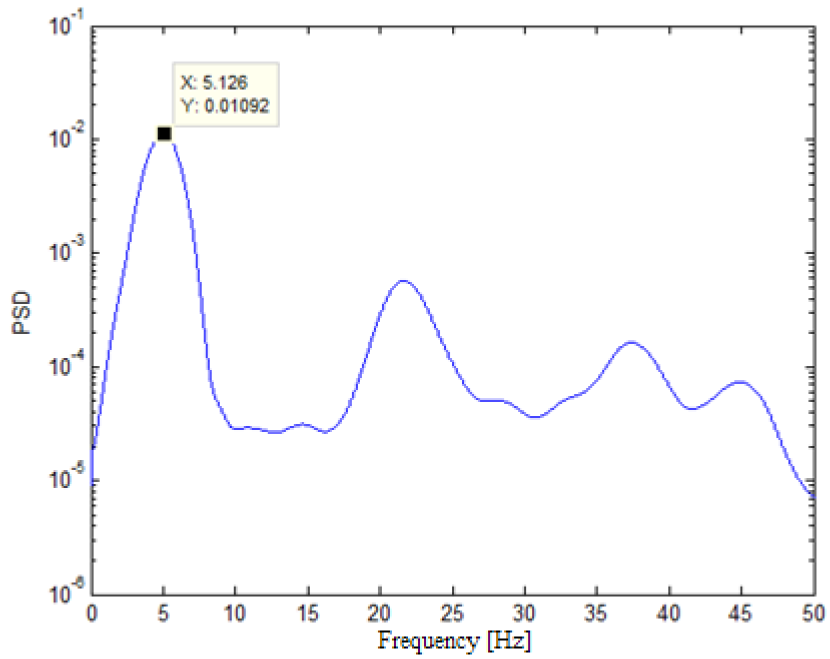

Figure 38. Flutter frequency of the 1/10 scaled F-16 wing like plate with 40 mm diameter aluminum store

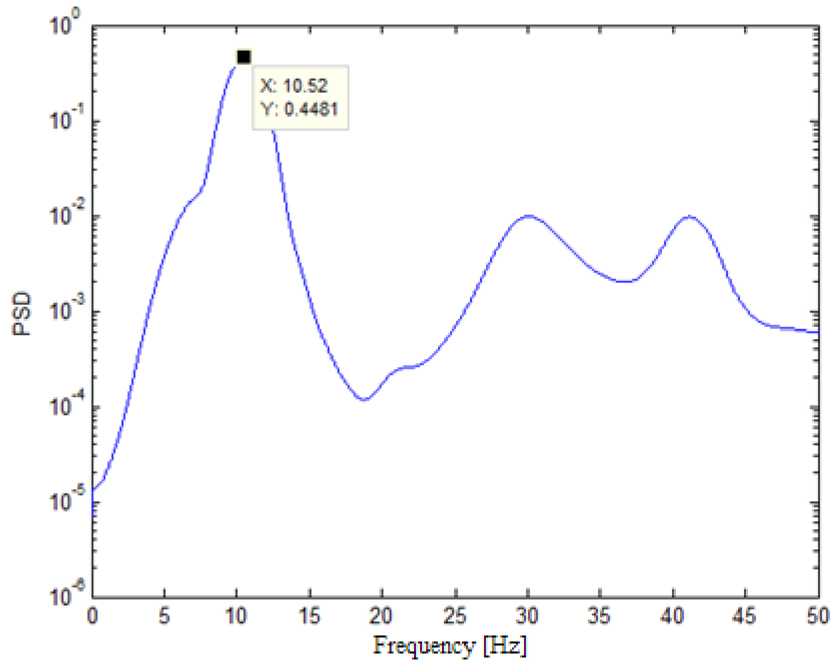

Figure 39. Flutter frequency of the 1/10 scaled F-16 wing like plate with 10 mm diameter steel store

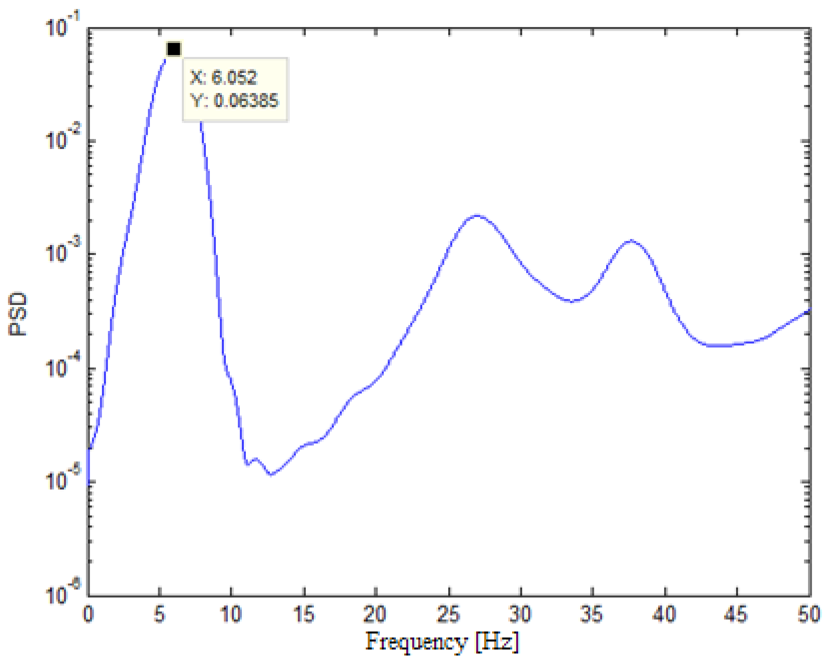

Figure 40. Flutter frequency of the 1/10 scaled F-16 wing like plate with 20 mm diameter steel store

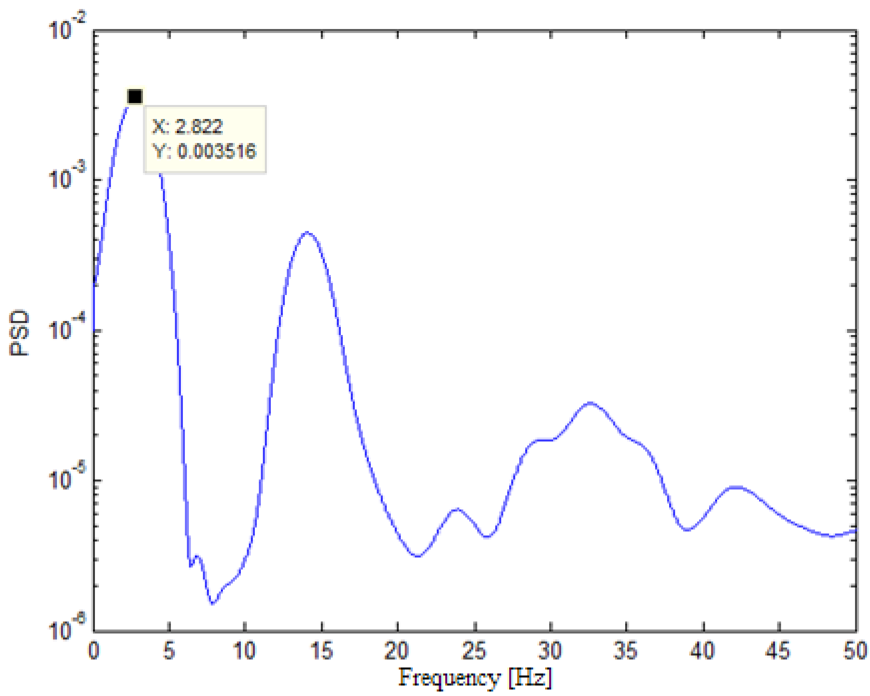

Figure 41. Flutter frequency of the 1/10 scaled F-16 wing like plate with 40 mm diameter steel store

Table 10. Wind tunnel flutter test results for the wing like plate combinations

Test #	Test Configuration	Flutter Speed (m/s)
1	1/10 scaled F-16 wing like plate	72.92
2	1/10 scaled F-16 wing like plate with 10 mm diameter aluminum store, W= 0.070 kg, I_z= 0.9286 kg.mm^2	69.97
3	1/10 scaled F-16 wing like plate with 20 mm diameter aluminum store, W= 0.300 kg, I_z= 14.8568 kg.mm^2	66.8
4	1/10 scaled F-16 wing like plate with 40 mm diameter aluminum store, W= 1.200 kg, I_z= 237.7089 kg.mm^2	61.56
5	1/10 scaled F-16 wing like plate with 10 mm diameter steel store, W= 0.224 kg, I_z= 2.7058 kg.mm^2	67.63
6	1/10 scaled F-16 wing like plate with 20 mm diameter steel store, W= 0.894 kg, I_z= 43.2935 kg.mm^2	64.61
7	1/10 scaled F-16 wing like plate with 40 mm diameter steel store, W= 3.576 kg, I_z= 692.6966 kg.mm^2	63.16

CHAPTER 6

DISCUSSION & CONCLUSION

This chapter is devoted the comparison of analysis results with test results. Firstly, results of two different solution methods, namely K-method and g-method, are compared with the test results. Then, two solution methods of ZAERO© are compared with each other. At the end of the chapter, planned future works are explained.

6.1. Comparison of Analysis and Test Results

This section compares the g-method and K-method solutions of ZAERO© with the wind tunnel test results.

6.1.1. Comparison of g-method Analysis Results with Test Results

Table 11 shows the comparison of the g-method flutter analysis results with the wind tunnel flutter test results for the rectangular plate. It is obvious that flutter speed estimation of ZAERO© for this case is in great agreement with the wind tunnel test results. Flutter frequency estimation is also at acceptable levels. ZAERO© estimates lower flutter speed than the wind tunnel test results. Therefore, it can be said that analysis results are conservative. Test system is highly simple and flutter is easily observed for this test item during the wind tunnel test. Due to this reason, flutter speed estimation for this test item is very accurate.

Table 12 shows the comparison of the g-method flutter analysis results with the wind tunnel flutter test results for the 1/10 scaled F-16 wing like plate. Flutter speed estimation of ZAERO© for this case is also lower than the wind tunnel test results, but the difference between the results gets larger. Flutter frequency estimation is in great agreement with the wind tunnel test. ZAERO© estimates lower flutter speed than the wind tunnel test. Therefore, it is concluded that results are conservative.

Table 11. Comparison of wind tunnel flutter test with flutter analysis for the rectangular plate

ZAERO©			Test		Difference [Speed] (%)	Difference [Frequency] (%)
Assumed Structural Damping	Flutter Speed (m/s)	Flutter Frequency (Hz)	Flutter Speed (m/s)	Flutter Frequency (Hz)		
%0	22.5	10.4	24.9	8.8	9.6	18.2
%0.5	22.6	10.3			9.2	17.0
%1	22.8	10.2			8.4	15.9
%1.5	23.0	10.2			7.6	15.9
%2	23.2	10.1			6.8	14.7
%2.5	23.3	10.0			6.4	13.6
%3	23.5	9.9			5.6	12.5
%3.5	23.7	9.8			4.8	11.4
%4	23.9	9.7			4.0	10.2

Table 12. Comparison of wind tunnel flutter test with flutter analysis for the 1/10 scaled F-16 wing like plate

ZAERO©			Test		Difference [Speed] (%)	Difference [Frequency] (%)
Assumed Structural Damping	Flutter Speed (m/s)	Flutter Frequency (Hz)	Flutter Speed (m/s)	Flutter Frequency (Hz)		
%0	56.3	16.4	73.0	18.02	22.9	9.0
%0.5	56.4	16.3			22.7	9.5
%1	56.6	16.3			22.5	9.5
%1.5	56.7	16.3			22.3	9.5
%2	56.8	16.2			22.2	10.0
%2.5	57.0	16.2			22.0	10.1
%3	57.1	16.1			21.8	10.65
%3.5	57.3	16.1			21.5	10.65
%4	57.4	16.0			21.4	11.21

Table 13 shows the comparison of the flutter analysis results with the wind tunnel flutter test results for the 1/10 scaled F-16 wing like plate with 10 mm diameter aluminum store. Flutter speed is lowered since the weight of the load on the wing is increased as expected. Flutter speed estimation of ZAERO© is lower than the wind tunnel test for this case, but the difference is again large. Flutter frequency estimation is also getting worse. As the load is increased on the plate, initial deflection of the wing is also increased during the wind tunnel test. Increased initial deflection resulted in worse estimation of flutter speed for the test item. This deflection is not taken into account in ZAERO© analysis. ZAERO© estimates lower flutter speed than the wind tunnel test. Therefore, it is concluded that results are on the conservative side.

Table 13. Comparison of wind tunnel flutter test with flutter analysis for the 1/10 scaled F-16 wing like plate with 10 mm diameter aluminium store

ZAERO©			Test		Difference [Speed] (%)	Difference [Frequency] (%)
Assumed Structural Damping	Flutter Speed (m/s)	Flutter Frequency (Hz)	Flutter Speed (m/s)	Flutter Frequency (Hz)		
%0	52.7	11.1	70.0	13.35	24.7	16.9
%0.5	53.7	11.0			23.3	17.6
%1	54.8	10.8			21.7	19.1
%1.5	55.7	10.7			20.4	20.0
%2	55.8	10.6			20.3	20.6
%2.5	55.9	10.6			20.1	20.6
%3	56.0	10.5			20.0	21.4
%3.5	56.1	10.5			19.9	21.4
%4	56.1	10.5			19.9	21.4

Similar results for the other configurations are also obtained. The results of other combinations are given in Appendix B.

Investigation of g-method flutter analysis results show that this solution method always give lower flutter speed than the wind tunnel flutter test. Due to this reason g-method flutter analysis results can be used as a guide to the flutter tests.

6.1.2. Comparison of K-method Analysis Results with Test Results

Table 14 shows the comparison of the flutter analysis results with the wind tunnel flutter test results for the rectangular plate. Both flutter speed and frequency results are closer to test results, and difference is very low for this case. Flutter speed estimation of ZAERO© for this case is lower than the wind tunnel test. Then, it is concluded that analysis results are over-conservative.

Table 14. Comparison of wind tunnel flutter test with flutter analysis for the rectangular plate

<table>
<tr><th colspan="3">ZAERO©</th><th colspan="2">Test</th><th rowspan="2">Difference [Speed] (%)</th><th rowspan="2">Difference [Frequency] (%)</th></tr>
<tr><th>Assumed Structural Damping</th><th>Flutter Speed (m/s)</th><th>Flutter Frequency (Hz)</th><th>Flutter Speed (m/s)</th><th>Flutter Frequency (Hz)</th></tr>
<tr><td>%0</td><td>23.8</td><td>9.7</td><td rowspan="9">24.9</td><td rowspan="9">8.8</td><td>4.4</td><td>10.2</td></tr>
<tr><td>%0.5</td><td>24.0</td><td>9.6</td><td>3.6</td><td>9.1</td></tr>
<tr><td>%1</td><td>24.2</td><td>9.5</td><td>2.8</td><td>8.0</td></tr>
<tr><td>%1.5</td><td>24.4</td><td>9.4</td><td>2.0</td><td>6.8</td></tr>
<tr><td>%2</td><td>24.6</td><td>9.3</td><td>1.2</td><td>5.7</td></tr>
<tr><td>%2.5</td><td>24.8</td><td>9.2</td><td>0.4</td><td>4.5</td></tr>
<tr><td>%3</td><td>25.0</td><td>9.1</td><td>0.4</td><td>3.4</td></tr>
<tr><td>%3.5</td><td>25.2</td><td>9.0</td><td>1.2</td><td>2.3</td></tr>
<tr><td>%4</td><td>25.4</td><td>8.9</td><td>2.0</td><td>1.1</td></tr>
</table>

Table 15 shows the comparison of the flutter analysis results with the wind tunnel flutter test results for the 1/10 scaled F-16 wing like. For this case, although flutter speed estimation is not close to test result, frequency results are very close to test results. Flutter speed estimation of ZAERO© for this case is lower than the wind tunnel test. Then, it is concluded that analysis results are over-conservative.

Table 15. Comparison of wind tunnel flutter test with flutter analysis for the 1/10 scaled F-16 wing like plate

ZAERO©			Test		Difference [Speed] (%)	Difference [Frequency] (%)
Assumed Structural Damping	Flutter Speed (m/s)	Flutter Frequency (Hz)	Flutter Speed (m/s)	Flutter Frequency (Hz)		
%0	51.0	17.7	73.0	18.02	30.1	1.8
%0.5	51.2	17.6			29.9	2.3
%1	51.4	17.5			29.6	2.9
%1.5	51.6	17.4			29.3	3.4
%2	51.8	17.4			29.0	3.4
%2.5	52.1	17.3			28.6	4.0
%3	52.3	17.2			28.4	4.6
%3.5	52.5	17.1			28.0	5.1
%4	52.7	17.0			27.8	5.7

Table 16 shows the comparison of the flutter analysis results with the wind tunnel flutter test results for the 1/10 scaled F-16 wing like plate with 10 mm diameter aluminum store. It is expected to have lower flutter speed than the only plate case. However it is seen that higher flutter speed is observed for this case, which indicates that there is an inconsistency for the solution of this method. There is no such an inconsistency in flutter frequency results. Flutter frequency is lowered as expected. For this case, differences between both flutter speed and flutter frequency are increased. Flutter speed estimation of ZAERO© for this case is lower than the wind tunnel test. Then, it is concluded that analysis results are over-conservative.

Table 16. Comparison of wind tunnel flutter test with flutter analysis for the 1/10 scaled F-16 wing like plate with 10 mm diameter aluminium store

ZAERO©			Test		Difference [Speed] (%)	Difference [Frequency] (%)
Assumed Structural Damping	Flutter Speed (m/s)	Flutter Frequency (Hz)	Flutter Speed (m/s)	Flutter Frequency (Hz)		
%0	53.0	11.1	70.0	13.35	24.3	16.9
%0.5	54.1	10.9			22.7	18.4
%1	55.1	10.7			21.3	19.9
%1.5	55.7	10.6			20.4	20.6
%2	55.7	10.6			20.4	20.6
%2.5	55.8	10.6			20.3	20.6
%3	55.9	10.5			20.1	21.4
%3.5	56.0	10.5			20.0	21.4
%4	56.1	10.4			19.9	22.1

Similar results for the other configurations are also obtained. The results of other combinations are given in Appendix C.

Results of K-method flutter analysis indicates that flutter speed increases as the plate is loaded with an external store. However, it is expected to have lower flutter speed when the plate is loaded with an external store as seen in wind tunnel flutter tests. Then, K-method flutter analysis are not suggested to be used as a guide to the flutter tests. Although, some of the K-method results are conservative, inconsistency in some other results make this solution method as an unreliable solution method.

6.2. Comparison of K-method and g-method Results

In K-method solution method a straightforward complex eigenvalue problem of each reduced frequency is solved. There are some drawbacks of K-method. Firstly, the solution is valid only at zero damping, other damping values are artificial. Artificial damping values may not have physical meaning. Secondly, in K-method solution technique flutter analysis is not performed at various air densities iteratively until the condition of $V_f = Ma_\infty$ is satisfied, called matched point solution. Another drawback is the loop of the frequency and damping values around themselves. This loop creates a multi-value frequency and damping as a function of velocity. Then, it becomes difficult to follow the eigenvalue in the reduced frequency list. Finally, K-method excludes the rigid body modes from its flutter equation since it cannot generate flutter solution at k = 0 [24].

When the results are investigated, it is seen that in some cases flutter frequency changes dramatically with the assumed structural damping. The reason is that, two different flutter mode is found for that case and as the assumed structural damping increases dominant flutter mode changes. If the difference between those flutter modes is too large, then it is seen in results that flutter frequency changes dramatically at consecutive assumed structural damping. This fact should be considered when evaluating the results.

Comparison of g-method and K-method analysis results with the wind tunnel flutter test shows that g-method analysis results are better to use in flutter analysis. Although, K-method gives more accurate estimation in some cases, it is seen that non-conservative results are also obtained in some other cases. Since the flutter tests are very critical tests, it is important to obtain a conservative result from the flutter analysis. Due to that reason, using g-method in flutter analysis is suggested.

6.3. Conclusion

As a result of this study, it is concluded that to be able to achieve a flutter analysis a modal experiment should be conducted in order to verify the modal data. It is sufficient to use modal analysis results for simple structures. However, flutter analysis needs to be conducted for more complex structures. For that reason, a modal experiment becomes necessary in those analysis.

g-method solution of ZAERO© is found to be more accurate than the K-method solution. g-method results are on the conservative side which is very critical in flutter tests since flutter tests are conducted for critical conditions for the fighter aircrafts.

Another important conclusion is that, flutter experiments should also be conducted even if a perfect flutter analysis is achieved. Too many unknowns exist since flutter is not a straightforward phenomenon. These unknowns can be eliminated only with experiments.

6.4. Future Work

After that, it is expected to apply all of the flutter certification procedures to a 1/6 scaled F-16 model aircraft. For that case, real time flutter estimation is going to be done by using the flutter estimation software during the wind tunnel test. Also, a flutter excitation system is going to be used to excite if there exists a flutter mode at lower speeds. At model F-16 case, modal test result is going to be used for flutter analysis and this result is going to be compared with the modal updated flutter analysis results.

REFERENCES

[1] M. H. Hansen. Aeroelastic instability problems for wind turbines. *Wind Energy*, 10(6), 2007.

[2] Y. C. Fung. *An Introduction to the Theory of Aeroelasticity*. Courier Dover Publications, May 2002.

[3] Lanchester, F.W.: “Torsional vibration of the Tail of an Aeroplane”, Aeronaut.Research Com.R & M.276, part i , 1916

[4] Bairstow, L., and A.Fage: “Oscillations of the Tail Plane and Body of an Aeroplane in Flight”, Aeronaut.Research Com.R & M.276, part ii, 1916

[5] Blasius, H.: “Über Schwingungserscheinungen an Einholmigen Unterflügeln”, Z. Flugtech. u. Motorluftschif. 16. 39-42, 1925

[6] Smilg, B.: “The Instability of Pitching Oscillations of an Airfoil in Subsonic Incompressible Potential Flow”, J.Aeronaut.Sci.16,691-696 , 1949

[7] Cheilik, H., and H.Frissel: “Theoretical Criteria for Single Degree of Freedom Flutter at Supersonic Speeds”, Cornell Aeronaut.Lab.Rept.CAL-7A , May 1947

[8] Runyan, H.L., H. J. Cunningham, and C.E.Watkins: “Theoretical Investigation of Several Types of Single-Degree-of-Freedom Flutter”, J.Aeronaut.Sci.19, 101-110, 126 , 1952 Comments by K.P.Abichandani and R.M.Rosenberg and author.s reply, 215-216; 503-504

[9] Cunningham, H.J.: “Analysis of Pure-Bending Flutter of a Cantilever Swept Wing and Its Relation to Bending-Torsion Flutter”, NACA Tech.Note 2461 , 1951

[10] Greidanus, J.H.: “Low-Speed Flutter”, J.Aeronaut.Sci.16,127-128 , 1949

[11] Dugundji, J.: “Theoretical consideration of Panel flutter at high supersonic Mach No.”, AIAA J. Vol.4, No.7, 1966

[12] E.H.Dowell, “Non linear oscillation of a fluttering plate”, AIAA J. Vol.4,No.7, 1996.

[13] E.H.Dowell, “Theoretical and experimental panel flutter study”, AIAA J. Vol.3,No.12, 1995.

[14] J.B.Kosmatka, “Flexure-Torsion behavior of prismatic beam”, AIAA J. Vol.31,No.1, 1993.

[15] Libo, W., Long, S., Lei, C., Zhigang, W., Chao, Y., “Design and Analysis of a Wind Tunnel Test Model System for Gust Alleviation of Aeroelastic Aircraft”, 53rd AIAA/ASME/ASCE/AHS/ASC Structures, Structural Dynamics and Materials Conference, 23 - 26 April 2012, Honolulu, Hawaii

[16] Neal, D. A., Good, M. G., Johnson, C. O., Robertshaw, H.H., Mason, W. H., Inman, D. J., “Design and Wind-Tunnel Analysis of a Fully Adaptive Aircraft Configuration”, 45th AIAA/ASME/ASCE/AHS/ASC Structures, Structural Dynamics & Materials Conference 19 - 22 April 2004, Palm Springs, California

[17] Omar, A.A., Kurban, A., “Design, Fabrication and Experimental Testing of IIUM Free Wing Unmanned Aerial Vehicle (IIUM-FWUAV)”, Australian Journal of Basic and Applied Sciences, 5(6): 381-389, 2011 ISSN 1991-8178

[18] Samikkannu R.. “Wind Tunnel Flutter Testing of Composite T-Tail Model of a Transport Aircraft with Fuselage Flexibility”, Wind Tunnels and Experimental Fluid Dynamics Research, Prof. Jorge Colman Lerner (Ed.), ISBN: 978-953-307-623-2, InTech, 2011 Available from: http://www.intechopen.com/books/wind-tunnels-andexperimental-fluid-

dynamics-research/wind-tunnel-flutter-testing-of-composite-t-tail-model-of-a-transportaircraft-with-fuselage-flexibil

[19] Strand, T., Levinsky, E.S., Wind Tunnel Tests of a Free-Wing Tilt-Propeller V/Stol Airplane Model, Aeronautical Research Report, October 1969

[20] Gloth, G., Degener, M., Füllekrug, U., Gschwilm, J., Sinapius, M., Fargette, P., Levadoux, B., Lubrina, P.: “New Ground Vibration Testing Techniques for Large Aircraft”, Sound and Vibration, Vol. 35, No. 11, pp. 14- 18, 2001

[21] Göge, D., Böswald, M., Füllekrug, U., Lubrina, P.: “Ground Vibration Testing of Large Aircraft – State-of-the-Art and Future Perspectives”, IMAC 25 Int.Modal Analysis Conf., Orlando, FL, Feb. 2007.

[22] Kehoe, M. W., A Historical Overview of Flight Flutter Testing, NASA Technical Memorandum 4720, October 1995.

[23] Ewins, D.J., Modal Testing: Theory, Practice and Application, Research Studies Press Ltd., Baldock, Hertfordshire, England, 2000.

[24] ZAERO© Theoretical Manual, Version 8.5, ZONA 02 – 12.4, 2011

APPENDIX A

COMPARISON OF MODAL ANALYSIS RESULTS WITH MODAL TEST RESULTS FOR DIFFERENT EXTERNAL STORE CONFIGURATIONS

Table 17. Natural frequencies of 1/10 scaled F-16 wing like plate with 20 mm diameter aluminum external store

Mode no	Frequency (Hz) First boundary condition	Frequency (Hz) Second boundary condition	Frequency (Hz) Modal test
1	3.94	5.11	3.94
2	10.93	12.57	12.49
3	25.36	32.60	27.73
4	33.46	45.58	41.15
5	42.83	67.45	58.45
6	61.03	72.36	61.54
7	90.47	108.52	88.35
8	103.88	120.5	94.93
9	105.34	149.98	-
10	131.69	163.35	-

Table 18. Natural frequencies of 1/10 scaled F-16 wing like plate with 40 mm diameter aluminum external store

Mode no	Frequency (Hz) First boundary condition	Frequency (Hz) Second boundary condition	Frequency (Hz) Modal test
1	2.15	2.69	2.28
2	6.20	6.90	6.72
3	21.37	27.43	20.50
4	31.73	42.46	39.21
5	41.73	63.94	59.56
6	55.93	88.15	71.11
7	60.44	91.97	88.89
8	87.27	92.90	95.66
9	92.83	113.82	120.04
10	124.84	150.02	-

Table 19. Natural frequencies of 1/10 scaled F-16 wing like plate with 10 mm diameter steel external store

Mode no	Frequency (Hz) First boundary condition	Frequency (Hz) Second boundary condition	Frequency (Hz) Modal test
1	4.36	5.70	4.38
2	12.16	14.15	14.42
3	26.26	33.53	29.04
4	33.93	46.04	42.35
5	43.0	67.95	58.86
6	61.77	72.39	62.95
7	90.38	108.92	90.08
8	105.17	122.05	100.33
9	114.8	148.46	-
10	132.37	149.91	-

Table 20. Natural frequencies of 1/10 scaled F-16 wing like plate with 20 mm diameter steel external store

Mode no	Frequency (Hz) First boundary condition	Frequency (Hz) Second boundary condition	Frequency (Hz) Modal test
1	2.60	3.32	2.68
2	7.15	8.01	8.10
3	23.28	30.53	25.29
4	32.46	44.76	47.92
5	42.50	66.81	60.03
6	59.45	89.06	65.21
7	72.32	107.52	89.69
8	89.96	113.78	97.64
9	101.18	119.11	125.05
10	130.32	150.84	-

Table 21. Natural frequencies of 1/10 scaled F-16 wing like plate with 40 mm diameter steel external store

Mode no	Frequency (Hz) First boundary condition	Frequency (Hz) Second boundary condition	Frequency (Hz) Modal test
1	1.37	1.73	1.29
2	3.76	4.15	4.07
3	20.74	26.49	14.56
4	31.77	42.21	25.99
5	39.055	58.68	59.42
6	41.35	58.80	69.65
7	50.53	72.13	93.90
8	74.25	76.82	107.69
9	90.03	111.94	-
10	116.79	120.68	-

68

APPENDIX B

FLUTTER ANALYSIS RESULTS FOR THE 1/10 SCALED F-16 WING LIKE PLATE

Table 22. Flutter analysis results for the 1/10 scaled F-16 wing like plate with a 20 mm diameter aluminum store

Structural damping [G]	0.0%	0.50%	1.0%	1.5%	2.0%	2.5%	3.0%	3.5%	4.0%
Speed [m/s] g-method	49.6	52.8	55.6	57.6	59.7	60.0	60.1	60.2	60.3
Frequency [Hz] g-method	31.0	30.6	30.4	30.2	30.0	7.7	7.7	7.7	7.7
Speed [m/s] K-method	59.4	59.5	59.6	59.7	59.8	59.9	60.0	60.1	60.1
Frequency [Hz] K-method	7.8	7.7	7.7	7.6	7.5	7.5	7.4	7.4	7.3

Table 23. Flutter analysis results for the 1/10 scaled F-16 wing like plate with a 40 mm diameter aluminum store

Structural damping [G]	0.0%	0.50%	1.0%	1.5%	2.0%	2.5%	3.0%	3.5%	4.0%
Speed [m/s] g-method	52.3	54.2	55.7	56.8	57.8	58.9	60.0	60.1	61.6
Frequency [Hz] g-method	28.5	28.2	28.0	27.9	27.7	27.6	27.4	27.4	27.3
Speed [m/s] K-method	67.0	67.2	67.3	67.3	67.4	67.5	67.6	67.7	67.8
Frequency [Hz] K-method	4.2	4.1	4.1	4.1	4.1	4.1	4.1	4.1	4.1

Table 24. Flutter analysis results for the 1/10 scaled F-16 wing like plate with a 10 mm diameter steel store

Structural damping [G]	0.0%	0.50%	1.0%	1.5%	2.0%	2.5%	3.0%	3.5%	4.0%
Speed [m/s] g-method	51.4	55.3	58.1	60.7	61.6	61.7	61.8	61.9	62.0
Frequency [Hz] g-method	31.4	31.0	30.7	30.5	8.5	8.5	8.5	8.5	8.5
Speed [m/s] K-method	60.8	61.0	61.0	61.0	61.1	61.1	61.1	61.1	61.2
Frequency [Hz] K-method	8.5	8.4	8.3	8.3	8.3	8.2	8.2	8.1	8.1

Table 25. Flutter analysis results for the 1/10 scaled F-16 wing like plate with a 20 mm diameter steel store

Structural damping [G]	0.0%	0.50%	1.0%	1.5%	2.0%	2.5%	3.0%	3.5%	4.0%
Speed [m/s] g-method	45.8	48.7	50.9	52.6	54.3	55.7	57.0	58.2	59.4
Frequency [Hz] g-method	30.0	29.7	29.5	29.3	29.1	29.0	28.8	28.7	28.6
Speed [m/s] K-method	65.9	65.9	65.9	65.9	65.9	65.9	65.9	65.9	65.9
Frequency [Hz] K-method	5.0	5.0	5.0	5.0	4.9	4.9	4.9	4.9	4.9

Table 26. Flutter analysis results for the 1/10 scaled F-16 wing like plate with a 40 mm diameter steel store

Structural damping [G]	0.0%	0.50%	1.0%	1.5%	2.0%	2.5%	3.0%	3.5%	4.0%
Speed [m/s] g-method	54.5	55.8	56.9	58.1	59.2	60.2	60.9	61.6	62.3
Frequency [Hz] g-method	28.1	27.9	27.8	27.6	27.4	27.3	27.2	27.1	27.0
Speed [m/s] K-method	67.8	68.6	69.5	70.3	71.1	72.0	72.8	73.6	74.5
Frequency [Hz] K-method	2.6	2.6	2.6	2.6	2.6	2.6	2.6	2.6	2.6

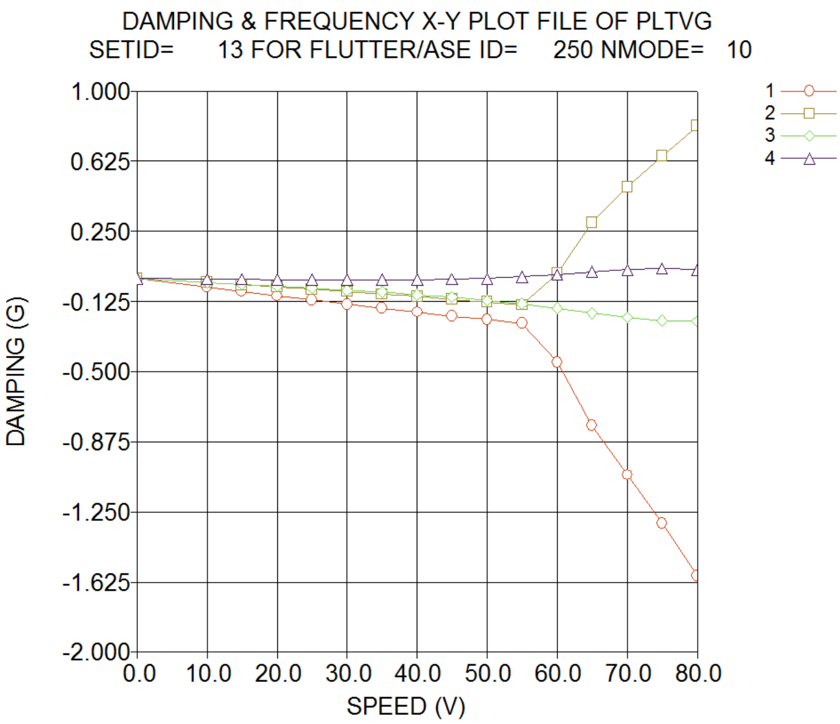

Figure 42. V-g plot of the 1/10 scaled F-16 wing like plate with a 20 mm diameter aluminum store

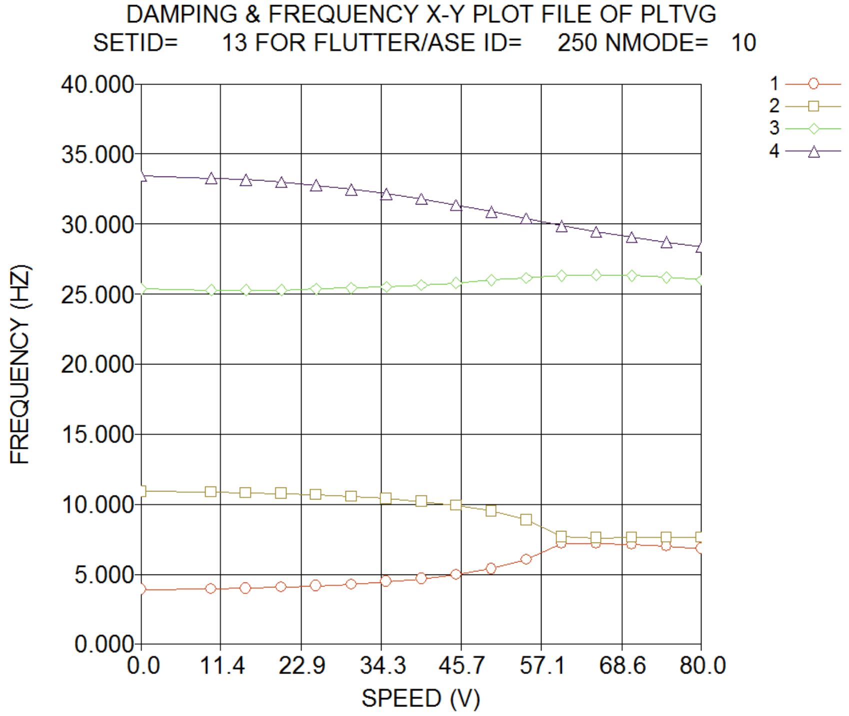

Figure 43. V-f plot of the 1/10 scaled F-16 wing like plate with a 20 mm diameter aluminum store

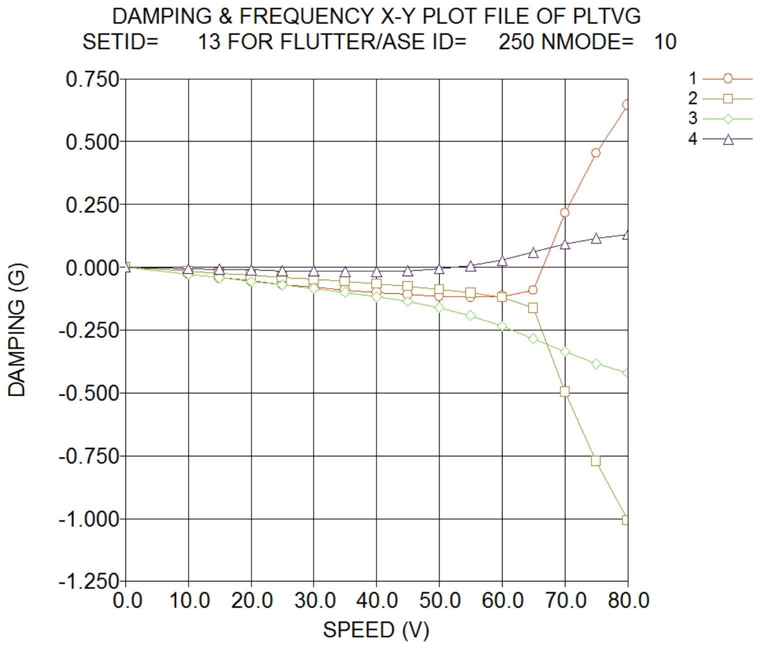

Figure 44. V-g plot of the 1/10 scaled F-16 wing like plate with a 40 mm diameter aluminum store

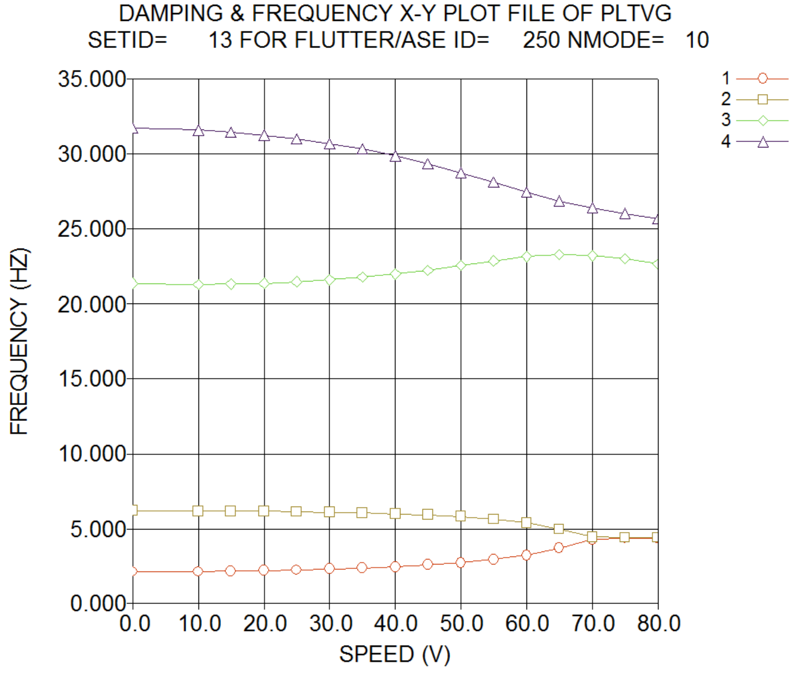

Figure 45. V-f plot of the 1/10 scaled F-16 wing like plate with a 40 mm diameter aluminum store

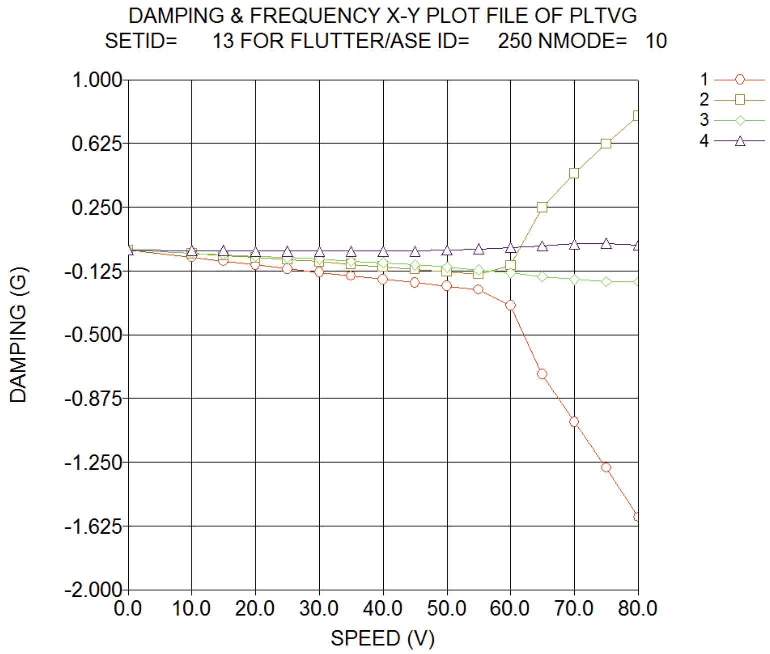

Figure 46. V-g plot of the 1/10 scaled F-16 wing like plate with a 10 mm diameter steel store

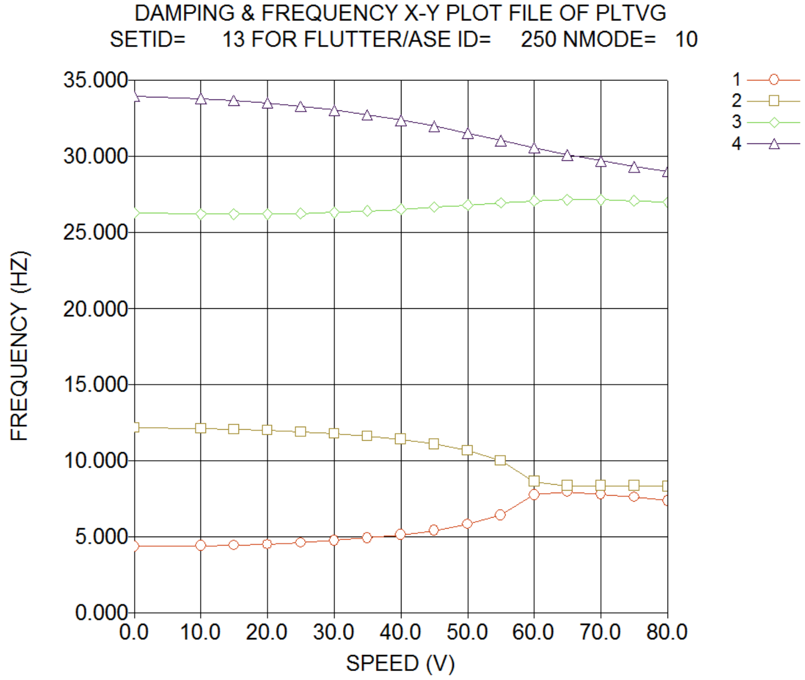

Figure 47. V-f plot of the 1/10 scaled F-16 wing like plate with a 10 mm diameter steel store

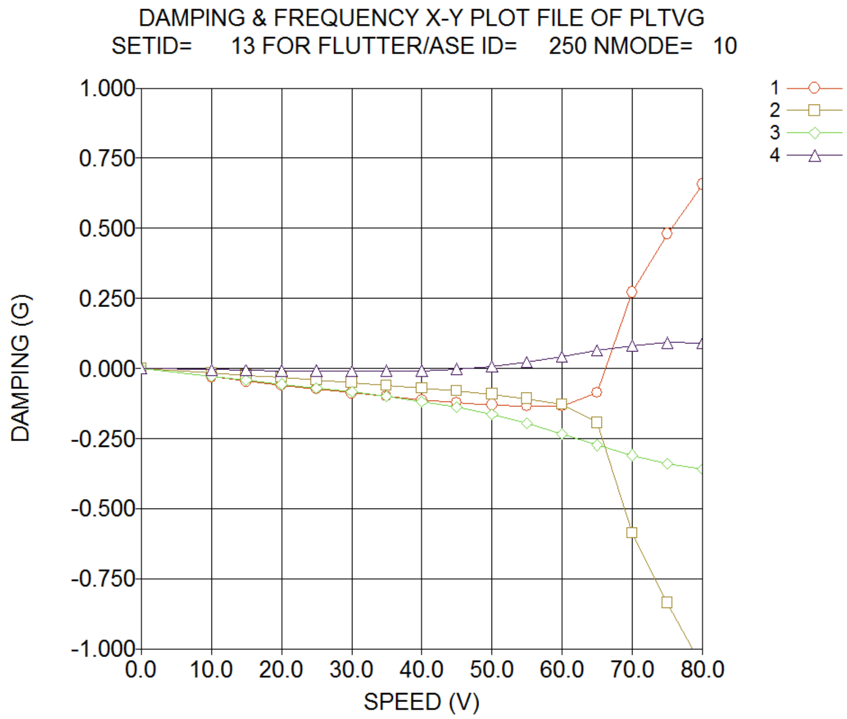

Figure 48. V-g plot of the 1/10 scaled F-16 wing like plate with a 20 mm diameter steel store

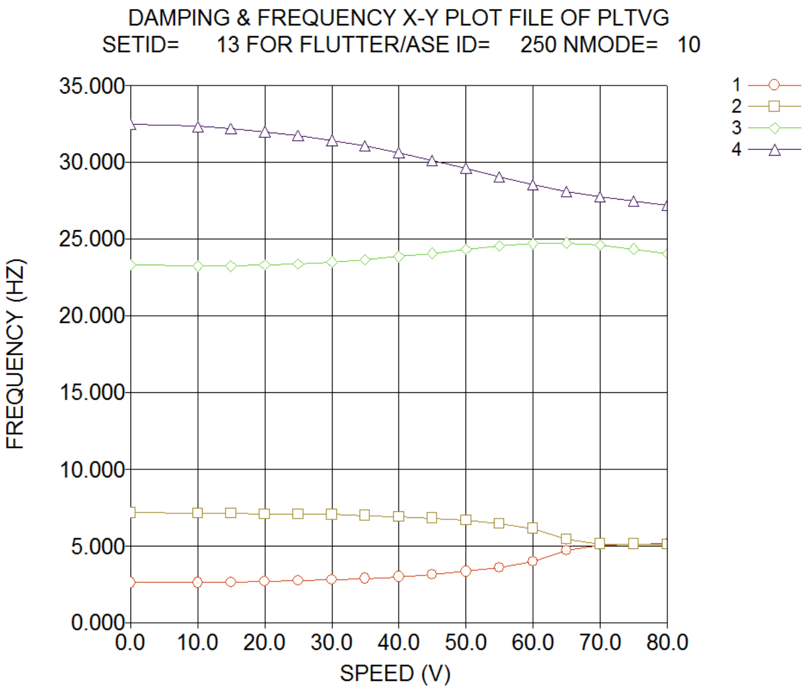

Figure 49. V-f plot of the 1/10 scaled F-16 wing like plate with a 20 mm diameter steel store

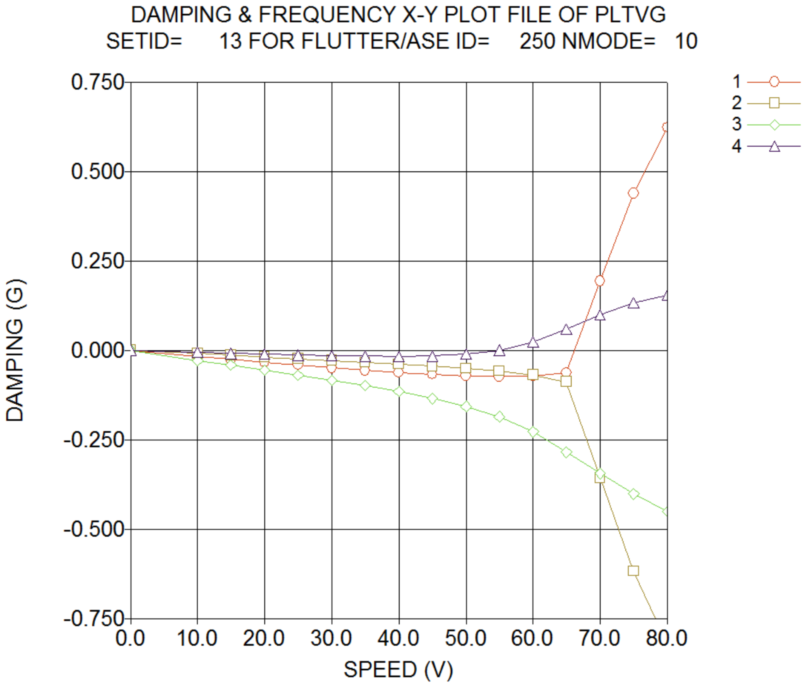

Figure 50. V-g plot of the 1/10 scaled F-16 wing like plate with a 40 mm diameter steel store

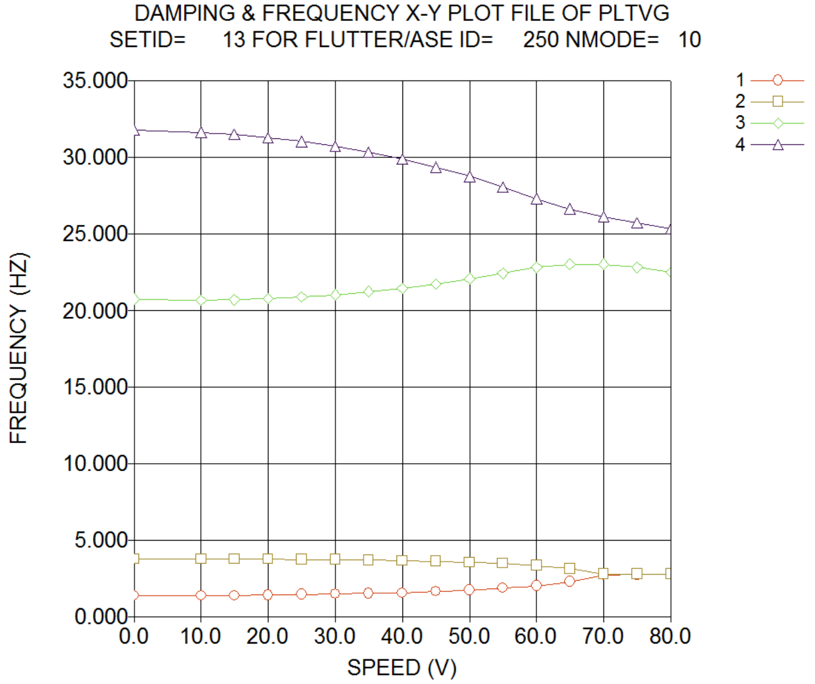

Figure 51. V-f plot of the 1/10 scaled F-16 wing like plate with a 40 mm diameter steel store

APPENDIX C

COMPARISON OF G-METHOD ANALYSIS RESULTS WITH TEST RESULTS

Table 27. Comparison of wind tunnel flutter test with flutter analysis for the 1/10 scaled F-16 wing like plate with 20 mm diameter aluminium

ZAERO©			Test		Difference [Speed] (%)	Difference [Frequency] (%)
Assumed Structural Damping	Flutter Speed (m/s)	Flutter Frequency (Hz)	Flutter Speed (m/s)	Flutter Frequency (Hz)		
%0	49.6	31.0	66.8	9.25	25.8	235.0
%0.5	52.8	30.6			21.0	230.8
%1	55.6	30.4			16.8	228.7
%1.5	57.6	30.2			13.8	226.5
%2	59.7	30.0			10.6	224.3
%2.5	60.0	7.7			10.2	16.8
%3	60.1	7.7			10.0	16.8
%3.5	60.2	7.7			9.9	16.8
%4	60.3	7.7			9.7	16.8

Table 28. Comparison of wind tunnel flutter test with flutter analysis for the 1/10 scaled F-16 wing like plate with 40 mm diameter aluminium store

ZAERO©			Test		Difference [Speed] (%)	Difference [Frequency] (%)
Assumed Structural Damping	Flutter Speed (m/s)	Flutter Frequency (Hz)	Flutter Speed (m/s)	Flutter Frequency (Hz)		
%0	52.3	28.5	61.6	5.0	15.1	470.0
%0.5	54.2	28.2			12.0	464.0
%1	55.7	28.0			9.6	460.0
%1.5	56.8	27.9			7.8	458.0
%2	57.8	27.7			6.2	454.0
%2.5	58.9	27.6			4.4	452.0
%3	60.0	27.4			2.6	448.0
%3.5	60.1	27.4			2.4	448.0
%4	61.6	27.3			0.0	446.0

Table 29. Comparison of wind tunnel flutter test with flutter analysis for the 1/10 scaled F-16 wing like plate with 10 mm diameter steel store

ZAERO©			Test		Difference [Speed] (%)	Difference [Frequency] (%)
Assumed Structural Damping	Flutter Speed (m/s)	Flutter Frequency (Hz)	Flutter Speed (m/s)	Flutter Frequency (Hz)		
%0	51.4	31.4	67.6	10.55	24.0	197.6
%0.5	55.3	31.0			18.2	193.8
%1	58.1	30.7			14.1	191.0
%1.5	60.7	30.5			10.2	189.1
%2	61.6	8.5			8.9	19.4
%2.5	61.7	8.5			8.7	19.4
%3	61.8	8.5			8.6	19.4
%3.5	61.9	8.5			8.4	19.4
%4	62.0	8.5			8.3	19.4

Table 30. Comparison of wind tunnel flutter test with flutter analysis for the 1/10 scaled F-16 wing like plate with 20 mm diameter steel store

ZAERO©			Test		Difference [Speed] (%)	Difference [Frequency] (%)
Assumed Structural Damping	Flutter Speed (m/s)	Flutter Frequency (Hz)	Flutter Speed (m/s)	Flutter Frequency (Hz)		
%0	45.8	30.0	64.6	6.0	29.1	400.0
%0.5	48.7	29.7			24.6	395.0
%1	50.9	29.5			21.2	391.7
%1.5	52.6	29.3			18.6	388.3
%2	54.3	29.1			15.9	385.0
%2.5	55.7	29.0			13.8	383.3
%3	57.0	28.8			11.8	380.0
%3.5	58.2	28.7			9.9	378.3
%4	59.4	28.6			8.1	376.7

Table 31. Comparison of wind tunnel flutter test with flutter analysis for the 1/10 scaled F-16 wing like plate with 40 mm diameter steel store

ZAERO©			Test		Difference [Speed] (%)	Difference [Frequency] (%)
Assumed Structural Damping	Flutter Speed (m/s)	Flutter Frequency (Hz)	Flutter Speed (m/s)	Flutter Frequency (Hz)		
%0	54.5	28.1	63.2	2.9	13.8	869.0
%0.5	55.8	27.9			11.7	862.1
%1	56.9	27.8			10.0	858.6
%1.5	58.1	27.6			8.1	851.7
%2	59.2	27.4			6.3	844.8
%2.5	60.2	27.3			4.8	841.4
%3	60.9	27.2			3.6	837.9
%3.5	61.6	27.1			2.5	834.5
%4	62.3	27.0			1.4	831.0

APPENDIX D

COMPARISON OF K-METHOD ANALYSIS RESULTS WITH TEST RESULTS

Table 32. Comparison of wind tunnel flutter test with flutter analysis for the 1/10 scaled F-16 wing like plate with 20 mm diameter aluminium store

ZAERO©			Test		Difference [Speed] (%)	Difference [Frequency] (%)
Assumed Structural Damping	Flutter Speed (m/s)	Flutter Frequency (Hz)	Flutter Speed (m/s)	Flutter Frequency (Hz)		
%0	59.4	7.8	66.8	9.25	11.0	15.7
%0.5	59.5	7.7			10.9	16.8
%1	59.6	7.7			10.8	16.8
%1.5	59.7	7.6			10.6	17.8
%2	59.8	7.5			10.5	18.9
%2.5	59.9	7.5			10.3	18.9
%3	60.0	7.4			10.2	20.0
%3.5	60.1	7.4			10.0	20.0
%4	60.1	7.3			10.0	21.1

Table 33. Comparison of wind tunnel flutter test with flutter analysis for the 1/10 scaled F-16 wing like plate with 40 mm diameter aluminium store

ZAERO©			Test		Difference [Speed] (%)	Difference [Frequency] (%)
Assumed Structural Damping	Flutter Speed (m/s)	Flutter Frequency (Hz)	Flutter Speed (m/s)	Flutter Frequency (Hz)		
%0	67.0	4.2	61.6	5.0	8.8	16.0
%0.5	67.2	4.1			9.1	18.0
%1	67.3	4.1			9.3	18.0
%1.5	67.3	4.1			9.3	18.0
%2	67.4	4.1			9.4	18.0
%2.5	67.5	4.1			9.6	18.0
%3	67.6	4.1			9.7	18.0
%3.5	67.7	4.1			9.9	18.0
%4	67.8	4.1			10.1	18.0

Table 34. Comparison of wind tunnel flutter test with flutter analysis for the 1/10 scaled F-16 wing like plate with 10 mm diameter steel store

ZAERO©			Test		Difference [Speed] (%)	Difference [Frequency] (%)
Assumed Structural Damping	Flutter Speed (m/s)	Flutter Frequency (Hz)	Flutter Speed (m/s)	Flutter Frequency (Hz)		
%0	60.8	8.5	67.6	10.55	10.1	19.4
%0.5	61.0	8.4			9.8	20.4
%1	61.0	8.3			9.8	21.3
%1.5	61.0	8.3			9.8	21.3
%2	61.1	8.3			9.6	21.3
%2.5	61.1	8.2			9.6	22.3
%3	61.1	8.2			9.6	22.3
%3.5	61.1	8.1			9.6	23.2
%4	61.2	8.1			9.5	23.2

Table 35. Comparison of wind tunnel flutter test with flutter analysis for the 1/10 scaled F-16 wing like plate with 20 mm diameter steel store

ZAERO©			Test		Difference [Speed] (%)	Difference [Frequency] (%)
Assumed Structural Damping	Flutter Speed (m/s)	Flutter Frequency (Hz)	Flutter Speed (m/s)	Flutter Frequency (Hz)		
%0	65.9	5.0	64.6	6.0	2.0	16.7
%0.5	65.9	5.0			2.0	16.7
%1	65.9	5.0			2.0	16.7
%1.5	65.9	5.0			2.0	16.7
%2	65.9	4.9			2.0	18.3
%2.5	65.9	4.9			2.0	18.3
%3	65.9	4.9			2.0	18.3
%3.5	65.9	4.9			2.0	18.3
%4	65.9	4.9			2.0	18.3

Table 36. Comparison of wind tunnel flutter test with flutter analysis for the 1/10 scaled F-16 wing like plate with 40 mm diameter steel store

ZAERO©			Test		Difference [Speed] (%)	Difference [Frequency] (%)
Assumed Structural Damping	Flutter Speed (m/s)	Flutter Frequency (Hz)	Flutter Speed (m/s)	Flutter Frequency (Hz)		
%0	67.8	2.6	63.2	2.9	7.3	10.3
%0.5	68.6	2.6			8.5	10.3
%1	69.5	2.6			10.0	10.3
%1.5	70.3	2.6			11.2	10.3
%2	71.1	2.6			12.5	10.3
%2.5	72.0	2.6			13.9	10.3
%3	72.8	2.6			15.2	10.3
%3.5	73.6	2.6			16.5	10.3
%4	74.5	2.6			17.9	10.3

APPENDIX E

ZAERO© INPUT FILE FOR THE RECTANGULAR PLATE

```
$ NASTRAN input file created by the Patran 2010 64-Bit input file
$ translator on May      20, 2013 at 10:56:23.
$ Direct Text Input for Nastran System Cell Section
$ Direct Text Input for File Management Section
$ Direct Text Input for Executive Control
$ Normal Modes Analysis, Database
SOL 103
CEND
$ Direct Text Input for Global Case Control Data
TITLE = MSC.Nastran job created on 20-May-13 at 10:47:14
ECHO = SORT
RESVEC = NO
SUBCASE 1
$ Subcase name : Default
  SUBTITLE=Default
  METHOD = 1
  SPC = 2
  VECTOR(SORT1,REAL)=ALL
  SPCFORCES(SORT1,REAL)=ALL
BEGIN BULK
$ Direct Text Input for Bulk Data
PARAM    POST    0
PARAM   PRTMAXIM YES
EIGRL    1                       10      0
$ Elements and Element Properties for region : plaka_12_son
PSHELL   1       1      .005     1               1
$ Pset: "plaka_12_son" will be imported as: "pshell.1"
CQUAD4   1       1       1       2       6       5
CQUAD4   2       1       2       3       7       6
CQUAD4   3       1       3       4       8       7
CQUAD4   4       1       5       6       10      9
CQUAD4   5       1       6       7       11      10
CQUAD4   6       1       7       8       12      11
CQUAD4   7       1       9       10      14      13
CQUAD4   8       1       10      11      15      14
```

CQUAD4	9	1	11	12	16	15
CQUAD4	10	1	13	14	18	17
CQUAD4	11	1	14	15	19	18
CQUAD4	12	1	15	16	20	19
CQUAD4	13	1	17	18	22	21
CQUAD4	14	1	18	19	23	22
CQUAD4	15	1	19	20	24	23
CQUAD4	16	1	21	22	26	25
CQUAD4	17	1	22	23	27	26
CQUAD4	18	1	23	24	28	27
CQUAD4	19	1	25	26	30	29
CQUAD4	20	1	26	27	31	30
CQUAD4	21	1	27	28	32	31
CQUAD4	22	1	29	30	34	33
CQUAD4	23	1	30	31	35	34
CQUAD4	24	1	31	32	36	35
CQUAD4	25	1	33	34	38	37
CQUAD4	26	1	34	35	39	38
CQUAD4	27	1	35	36	40	39
CQUAD4	28	1	37	38	42	41
CQUAD4	29	1	38	39	43	42
CQUAD4	30	1	39	40	44	43
CQUAD4	31	1	41	42	46	45
CQUAD4	32	1	42	43	47	46
CQUAD4	33	1	43	44	48	47
CQUAD4	34	1	45	46	50	49
CQUAD4	35	1	46	47	51	50
CQUAD4	36	1	47	48	52	51
CQUAD4	37	1	49	50	54	53
CQUAD4	38	1	50	51	55	54
CQUAD4	39	1	51	52	56	55
CQUAD4	40	1	53	54	58	57
CQUAD4	41	1	54	55	59	58
CQUAD4	42	1	55	56	60	59
CQUAD4	43	1	57	58	62	61
CQUAD4	44	1	58	59	63	62
CQUAD4	45	1	59	60	64	63
CQUAD4	46	1	61	62	66	65
CQUAD4	47	1	62	63	67	66
CQUAD4	48	1	63	64	68	67
CQUAD4	49	1	65	66	70	69
CQUAD4	50	1	66	67	71	70
CQUAD4	51	1	67	68	72	71
CQUAD4	52	1	69	70	74	73
CQUAD4	53	1	70	71	75	74
CQUAD4	54	1	71	72	76	75
CQUAD4	55	1	73	74	78	77
CQUAD4	56	1	74	75	79	78

```
CQUAD4  57      1       75      76      80      79
CQUAD4  58      1       77      78      82      81
CQUAD4  59      1       78      79      83      82
CQUAD4  60      1       79      80      84      83
CQUAD4  61      1       81      82      86      85
CQUAD4  62      1       82      83      87      86
CQUAD4  63      1       83      84      88      87
CQUAD4  64      1       85      86      90      89
CQUAD4  65      1       86      87      91      90
CQUAD4  66      1       87      88      92      91
CQUAD4  67      1       89      90      94      93
CQUAD4  68      1       90      91      95      94
CQUAD4  69      1       91      92      96      95
$ Referenced Material Records
$ Material Record : PC
$ Description of Material : Date: 20-May-13           Time: 10:46:25
MAT1     1      2.1+9           .35     1200.
$ Nodes of the Entire Model
GRID     1              -.125   1.125   .005
GRID     2              -.0833331.125   .005
GRID     3              -.0416661.125   .005
GRID*    4                              1.11022-16      1.125
*       .005
GRID     5              -.125   1.08152 .005
GRID     6              -.0833331.08152 .005
GRID     7              -.0416661.08152 .005
GRID*    8                              1.06807-16      1.08152
*       .005
GRID     9              -.125   1.03804 .005
GRID     10             -.0833331.03804 .005
GRID     11             -.0416661.03804 .005
GRID*    12                             1.03741-16      1.03804
*       .005
GRID     13             -.125   .994565 .005
GRID     14             -.083333.994565 .005
GRID     15             -.041666.994565 .005
GRID*    16                             1.01715-16      .994565
*       .005
GRID     17             -.125   .951087 .005
GRID     18             -.083333.951087 .005
GRID     19             -.041666.951087 .005
GRID*    20                             1.0062-16       .951087
*       .005
GRID     21             -.125   .907609 .005
GRID     22             -.083333.907609 .005
GRID     23             -.041666.907609 .005
GRID*    24                             1.00346-16      .907609
*       .005
```

```
GRID     25             -.125   .86413  .005
GRID     26             -.083333.86413  .005
GRID     27             -.041666.86413  .005
GRID*     28                      1.00784-16      .86413
*       .005
GRID     29             -.125   .820652 .005
GRID     30             -.083333.820652 .005
GRID     31             -.041666.820652 .005
GRID*     32                      1.01824-16      .820652
*       .005
GRID     33             -.125   .777174 .005
GRID     34             -.083333.777174 .005
GRID     35             -.041666.777174 .005
GRID*     36                      1.03357-16      .777174
*       .005
GRID     37             -.125   .733696 .005
GRID     38             -.083333.733696 .005
GRID     39             -.041666.733696 .005
GRID*     40                      1.05274-16      .733696
*       .005
GRID     41             -.125   .690217 .005
GRID     42             -.083333.690217 .005
GRID     43             -.041666.690217 .005
GRID*     44                      1.07464-16      .690217
*       .005
GRID     45             -.125   .646739 .005
GRID     46             -.083333.646739 .005
GRID     47             -.041666.646739 .005
GRID*     48                      1.09818-16      .646739
*       .005
GRID     49             -.125   .603261 .005
GRID     50             -.083333.603261 .005
GRID     51             -.041666.603261 .005
GRID*     52                      1.12227-16      .603261
*       .005
GRID     53             -.125   .559783 .005
GRID     54             -.083333.559783 .005
GRID     55             -.041666.559783 .005
GRID*     56                      1.14581-16      .559783
*       .005
GRID     57             -.125   .516304 .005
GRID     58             -.083333.516304 .005
GRID     59             -.041666.516304 .005
GRID*     60                      1.16771-16      .516304
*       .005
GRID     61             -.125   .472826 .005
GRID     62             -.083333.472826 .005
GRID     63             -.041666.472826 .005
```

```
GRID*   64                      1.18687-16      .472826
*       .005
GRID    65              -.125   .429348 .005
GRID    66              -.083333.429348 .005
GRID    67              -.041666.429348 .005
GRID*   68                      1.2022-16       .429348
*       .005
GRID    69              -.125   .38587  .005
GRID    70              -.083333.38587  .005
GRID    71              -.041666.38587  .005
GRID*   72                      1.2126-16       .38587
*       .005
GRID    73              -.125   .342391 .005
GRID    74              -.083333.342391 .005
GRID    75              -.041666.342391 .005
GRID*   76                      1.21698-16      .342391
*       .005
GRID    77              -.125   .298913 .005
GRID    78              -.083333.298913 .005
GRID    79              -.041666.298913 .005
GRID*   80                      1.21425-16      .298913
*       .005
GRID    81              -.125   .255435 .005
GRID    82              -.083333.255435 .005
GRID    83              -.041666.255435 .005
GRID*   84                      1.2033-16       .255435
*       .005
GRID    85              -.125   .211957 .005
GRID    86              -.083333.211957 .005
GRID    87              -.041666.211957 .005
GRID*   88                      1.18304-16      .211957
*       .005
GRID    89              -.125   .168478 .005
GRID    90              -.083333.168478 .005
GRID    91              -.041666.168478 .005
GRID*   92                      1.15238-16      .168478
*       .005
GRID    93              -.125   .125    .005
GRID    94              -.083333.125    .005
GRID    95              -.041666.125    .005
GRID*   96                      1.11022-16      .125
*       .005
$ Loads for Load Case : Default
SPCADD   2       1
$ Displacement Constraints of Load Set : fixed
SPC1     1       123456  93      94      95      96
$ Referenced Coordinate Frames
ENDDATA 2a93dd26
```